AD-A074 162 STEVENS INST OF TECH HOBOKEN N J DAVIDSON LAB F/G 20/11
ANALYTICAL INVESTIGATION OF THE QUADRATIC FREQUENCY RESPONSE FO--ETC(U)
MAY 79 C H KIM, J F DALZELL N00014-78-C-0313
UNCLASSIFIED SIT-DL-79-9-2061 NL

| OF |
AD A074162

END
DATE FILMED
10-79
DDC

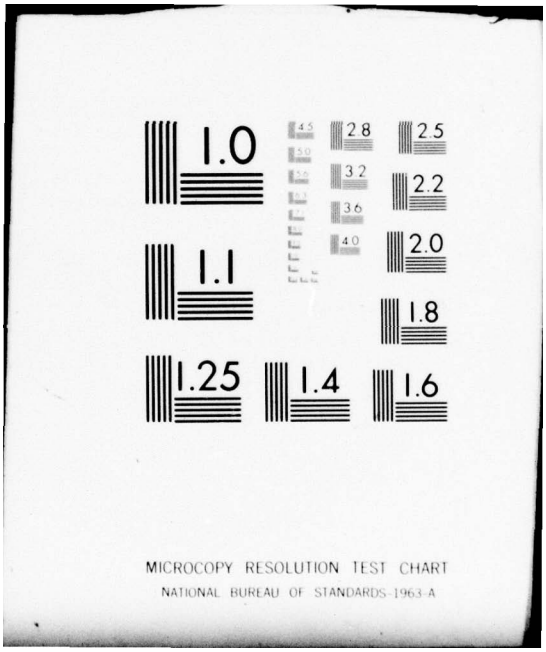
1.0
1.1
1.25
1.4
1.6
2.8
3.2
3.6
4.0
2.5
2.2
2.0
1.8
MICROCOPY RESOLUTION TEST CHART
NATIONAL BUREAU OF STANDARDS-1963-A

STEVENS INSTITUTE
OF TECHNOLOGY

CASTLE POINT STATION
HOBOKEN, NEW JERSEY 07030

R-2061

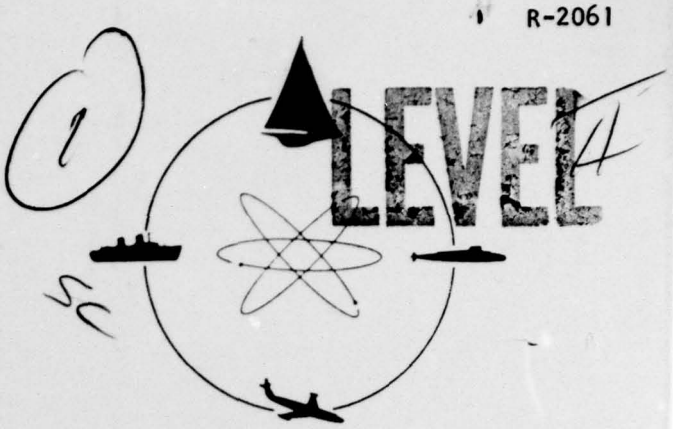

DAVIDSON LABORATORY

Report SIT-DL-79-9-2061

May 1979

ANALYTICAL INVESTIGATION OF THE QUADRATIC FREQUENCY RESPONSE FOR LATERAL DRIFTING FORCE AND MOMENT

by C.H. Kim and J.F. Dalzell

Sponsored by

Naval Sea Systems Command
General Hydromechanics Program
Administered by the David Taylor
Naval Ship Research & Development Center
Contract N00014-78-C-0313
DL Project 4605/042

UNCLASSIFIED

SECURITY CLASSIFICATION OF THIS PAGE (When Data Entered)

REPORT DOCUMENTATION PAGE	READ INSTRUCTIONS BEFORE COMPLETING FORM
1. REPORT NUMBER: SIT-DL-79-9-2061	2. GOVT ACCESSION NO.
3. RECIPIENT'S CATALOG NUMBER	
4. TITLE (and Subtitle): ANALYTICAL INVESTIGATION OF THE QUADRATIC FREQUENCY RESPONSE FOR LATERAL DRIFTING FORCE AND MOMENT.	5. TYPE OF REPORT & PERIOD COVERED: FINAL 15 March 1978 - May 1979
	6. PERFORMING ORG. REPORT NUMBER: SIT-DL-79-9-2061
7. AUTHOR(s): C.H. Kim and J.F. Dalzell	8. CONTRACT OR GRANT NUMBER(s): N00014-78-C-0313
9. PERFORMING ORGANIZATION NAME AND ADDRESS: Davidson Laboratory, Stevens Institute of Technology, Hoboken, NJ 07030	10. PROGRAM ELEMENT, PROJECT, TASK AREA & WORK UNIT NUMBERS: 12 81p.
11. CONTROLLING OFFICE NAME AND ADDRESS: David W. Taylor Naval Ship R&D Center, Bethesda, MD 20084 (Code 1505)	12. REPORT DATE: May 1979
	13. NUMBER OF PAGES: vii + 72 pp.
14. MONITORING AGENCY NAME & ADDRESS (if different from Controlling Office): Office of Naval Research, 800 N. Quincy Street, Arlington, VA 22217	15. SECURITY CLASS. (of this report): Unclassified
	15a. DECLASSIFICATION/DOWNGRADING SCHEDULE

16. DISTRIBUTION STATEMENT (of this Report)

APPROVED FOR PUBLIC RELEASE; DISTRIBUTION UNLIMITED.

17. DISTRIBUTION STATEMENT (of the abstract entered in Block 20, if different from Report)

18. SUPPLEMENTARY NOTES.

Sponsored by Naval Sea Systems Command, General Hydromechanics Program
Administered by the David Taylor Naval Ship Research & Development Center

19. KEY WORDS (Continue on reverse side if necessary and identify by block number)

Quadratic Frequency Response
Second-order Force
Lateral Drifting Force and Moment

20. ABSTRACT (Continue on reverse side if necessary and identify by block number)

Results of calculations are given for lateral drifting forces acting on a cylinder and a Series 60 hull derived by a new procedure involving application of the quadratic frequency response function (QFRF) and the close-fit method for flows induced by hull sections in the near field. The near field inductions are required by the QFRF in order to obtain the non-linear (second order) interaction effects in the presence of dual waves. This method yields the mean drifting force consisting of four components

(Cont'd)

DD FORM 1 JAN 73 1473 EDITION OF 1 NOV 65 IS OBSOLETE
S/N 0102-014-6601

UNCLASSIFIED
SECURITY CLASSIFICATION OF THIS PAGE (When Data Entered)

ABSTRACT (Cont'd)

of which the relative-wave-elevation term is dominant, whereas the Bernoulli quadratic term is secondary. A mathematical discontinuity of the drifting force in the neighborhood of a high frequency is investigated by applying a modified Green's function. Mean drifting forces for two forms have been calculated and the results compared with available analysis and model data. A fairly complete quadratic frequency response function for lateral drifting forces in the bi-frequency domain was computed for the Series 60 Ship C_B = 0.6 at sixty-degree heading. The computed results are presented in a three-dimensional view accompanied by a detailed discussion of the characteristic behavior.

C sub B

STEVENS INSTITUTE OF TECHNOLOGY
DAVIDSON LABORATORY
CASTLE POINT STATION
HOBOKEN, NEW JERSEY

Report SIT-DL-79-9-2061

May 1979

ANALYTICAL INVESTIGATION OF THE QUADRATIC FREQUENCY RESPONSE FOR LATERAL DRIFTING FORCE AND MOMENT

by C.H. Kim and J.F. Dalzell

Sponsored by

Naval Sea Systems Command
General Hydromechanics Program
Administered by the
David Taylor Naval Ship Research & Development Center
Contract N00014-78-C-0313
DL Project 4605/042

Reviewed by:

S. Tsakonas

S. Tsakonas
Chief, Fluid Dynamics Division

Approved:

John P. Breslin

John P. Breslin
Director

vii + 72 pp.

ABSTRACT

Results of calculations are given for lateral drifting forces acting on a cylinder and a Series 60 hull derived by a new procedure involving application of the quadratic frequency response function (QFRF) and the close-fit method for flows inducted by hull sections in the near field. The near field inductions are required by the QFRF in order to obtain the non-linear (second order) interaction effects in the presence of dual waves. This method yields the mean drifting force consisting of four components of which the relative-wave-elevation term is dominant, whereas the Bernoulli quadratic term is secondary. A mathematical discontinuity of the drifting force in the neighborhood of a high frequency is investigated by applying a modified Green's function. Mean drifting forces for two forms have been calculated and the results compared with available analysis and model data. A fairly complete quadratic frequency response function for lateral drifting forces in the bi-frequency domain was computed for the Series 60 Ship $C_B = 0.6$ at sixty-degree heading. The computed results are presented in a three-dimensional view accompanied by a detailed discussion of the characteristic behavior.

KEYWORDS

Quadratic Frequency Response

Second-order Force

Lateral Drifting Force and Moment

TABLE OF CONTENTS

NOMENCLATURE

a	wave amplitude
a_1, a_2 a_m, a_n	amplitude of wave component of frequency ω_1, ω_2, ω_m, ω_n
$\bar{A}_-$	wave amplitude ratio
B	beam of a section in the load waterplane
$c(x)$	a transverse section contour
C_F	non-dimensional lateral force coefficient (Eq.26)
C_M	non-dimensional lateral moment coefficient (Eq.27)
$D_w(t)$	drifting force
e	wave elevation (Eq.20)
$f(x)$	sectional lateral force
$\tilde{f}$	mean sectional lateral force
F	lateral force
$\tilde{F}$	mean lateral force
$g_1(t)$	linear impulse response
$g_2(t_1,t_2)$	second degree kernel analogous to an impulse response
G	pulsating source function
$G_1(\omega)$	linear frequency response function
$G_2(\omega_m,\pm\omega_n)$	quadratic frequency response function defined by Eq.(34)
h	wave height or wave elevation
$H_{1,k}(\omega_m,\pm\omega_n)$	functions defined by Eq.(32)
i	$\sqrt{-1}$
I_k	integral expression defined by Eq.(31)
L	hull length
$m_o(x)$	mass of a section
M	lateral moment
$\tilde{M}$	mean lateral moment

p	pressure
Q	source intensity
r	relative wave elevation
$S^{(m)}$	displacement of a response motion of mode m
S_j	segment
t	time
T	draft, period
x,y,z	moving body coordinates
X,Y,Z	space fixed coordinates
Δ	displacement
ν	wave number
ν_m	wave number of frequency ω_m
ρ	water density
φ	resultant velocity potential
$\Phi_D^{(m)}$	diffraction potential of mode m
$\Phi_R^{(m)}$	radiation potential of mode m
$\omega, \omega_m, \omega_n, \omega_1, \omega_2$	circular frequency
Ω_1, Ω_2	circular frequency
σ	non-dimensional frequency
τ	non-dimensional time

INTRODUCTION

The ultimate goal of the present study is to establish an improved prediction technique of the fluctuating lateral drifting force and moment (or second-order yaw moment) and then to determine their statistical characteristics. Thus, a useful tool would be available for prediction of the behavior of naval vessels in random seas.

The broad problem is divided into two Phases: Phase I provides an analysis and limited correlation with model measurements of mean drifting force; Phase II was proposed to be directed to a complete experimental determination of the QFRF and subsequent correlation with the theoretical predictions evolved in Phase I. This report deals only with Phase I.

A recent investigation[1] of the quadratic frequency response for added resistance has shown satisfactory agreement with the results of an experimental investigation.[2] Reference 2 shows that the quadratic response function can be utilized to predict reliably the very low-frequency, fluctuating added resistance in irregular waves. The analytical technique developed in these studies[1,2] has been applied by Kim and Breslin[3] for prediction of slow drift oscillation of a moored ship in random head seas. This method will be employed in the present investigation.

Simplified analytical methods have been proposed by Hsu and Blenkarn,[4] Newman,[5] and Faltinsen and Loken,[6] for the prediction of slow drift oscillation. These procedures depend on the mean drifting force, which represents only a special output from DRFR procedures.

Maruo[7] provided a basis for predicting the mean drifting force due to a monochromatic wave on a cylinder floating in a beam wave train. Ogawa[8] applied Maruo's method to a fixed ship by using a strip method based on the concept of the snake-type wave generator. He showed that his calculation agreed well with his experiments. Spens and Lalangas[9] reported experimental results on the mean lateral drifting force and moment on a ship model in

[1] Superior numbers in text matter refer to similarly numbered references listed at the end of this report.

oblique waves. Newman[10] calculated the mean lateral drifting force based on the slender body theory. However, his predictions did not agree well with the experiments.[9] Kim, et al,[11] calculated the mean lateral drifting force and moment on a fixed as well as a free ship in oblique waves, using a strip method and showed acceptable comparisons with experiments.[8,12] Salvesen[13] developed a method of calculating the mean added resistance and mean lateral drifting force by using a strip method. Compared with the results of Spens and Lalangas,[9] his results showed an appreciable discrepancy He attributed this discrepancy to difficulties encountered in the experiment and to "weak scatter" assumptions made in Newman's theory.[10]

Pinkster and Oortmerssen[14] applied a three-dimensional source distribution method to the evaluation of the mean drift forces, which were obtained by integrating the pressure distribution on the wetted hull surface.

The present calculations are carried out in two steps: (A) calculation of the lateral second-order force acting on a ship section, free or fixed in regular beam waves, and (B) stripwise calculation of the quadratic frequency response function for the ship in oblique dual waves. The analysis is based on the hypothesis that the contribution of the second-order potential to the second-order force is negligible compared to those contributed by the first-order potential. Rigorous analyses of the second-order force and moment on a cylinder free in waves have been given by Potash[15] and Söding,[16] both of which do not neglect the second-order potential. Faltinsen and Loken[6] also estimated the second-order potential in their evaluations of the slow drifting force and moment.

The present analysis integrates the pressure distribution on the section surface (as in Reference 14), whereas Maruo[7] integrates pressures over control surface in the far field. The former method may therefore be designated as a "near-field method," while the latter, a "far-field method."

The far-field method[7] yields a simple formula for the mean force whereas the near-field method presents a sum of several components. The latter seems to be complicated at first and difficult to use; however, it clearly reveals the effects of the behavior of the response motions such as heave and roll resonances and body parameters. Effects of motions and body parameters have remained unknown and sought after for many years by researchers. Moreover,

the far-field method cannot be used for the analysis of the quadratic frequency response for the drifting force and moment.

A two-dimensional procedure, mentioned above, has been employed as in Reference 11, for stripwise calculation of the force and moment of a ship in oblique dual waves.

A special output of the quadratic frequency procedure is, in fact, the mean drift force or moment as demonstrated later. Numerical calculations of the mean drifting force and moment have been carried out for a cylindrical model, tested by Koterayama,[17] and for a ship Series 60, C_B=0.6 by Lalangas.[12] The present analysis has been compared with the calculation by Maruo's method and model test data. Excellent agreement between the two methods has been confirmed for the bodies in beam seas. In oblique seas, however, the two analytical methods appear to be in good agreement.

The mean drifting force or moment consists of four components, i.e., gyroscopic-coupling,[force rate] x [displacement], the Bernoulli's quadratic, and the relative wave terms.

A highlight of the analysis of the components shows that the relative wave-induced drifting force component is the most dominant, seconded only by Bernoulli's quadratic pressure-induced term. In addition, the influence of the peak hull displacements on the component forces have been clearly observed. The presence of a mathematical discontinuity at a high frequency has been investigated by employing Ogilvie-Shin's modified Green's function.[18]

The quadratic frequency response functions for drifting force and moment of ship Series 60, C_B=0.6 have been calculated at a sixty-degree heading and the results are illustrated in a three-dimensional view (Figure 6).

The successful application of the quadratic frequency procedure which yields the mean drifting forces (and moments) as a specialized output lends support to the validity of the technique. Further confirmation of the utility of this procedure for elucidation of the bi-frequency domain characteristics of the entire QFRF (as described in Phase II in Davidson Laboratory Proposal P-1713R) requires model measurements currently unavailable.

THE INPUT-OUTPUT MODEL

A few definitions and relations pertaining to the general input-output model are needed in the present work. These will be given here for convenience, although they may be found in Reference 2 in greater detail.

The general input-output model is a time domain model and is written as:

$$F_w(t) = \int g_1(t_1)\eta(t-t_1)dt_1 + \iint g_2(t_1,t_2)\eta(t-t_1)\eta(t-t_2)dt_1\,dt_2 \qquad (1)$$

(Omission of limits on the integrals signifies limits of $\pm\infty$.)

In Eq. (1): $F_w(t)$ is the force or moment exerted by the waves

$\eta(t)$ is a suitably chosen wave elevation (a zero mean input)

$g_1(t)$ is a linear impulse response

$g_2(t_1,t_2)$ is a second degree kernel analogous to an impulse response

With respect to application to drifting force and moment, the ship is assumed to be station-keeping in a wave system (the input) which is defined as the wave elevation at a point stationary with respect to the mean position of the ship. The second degree kernel is assumed to be symmetric in its arguments, and both kernels are assumed smooth and absolutely integrable.

The first term in Eq.(1) is the ordinary linear convolution of a linear impulse response function $g_1(t_1)$ with $\eta(t)$. The second term is a double convolution, and the second degree kernel $g_2(t_1,t_2)$ might be called a quadratic impulse response. According to basic assumptions, the two impulse responses are related to the linear and quadratic frequency response functions by Fourier transforms. These two sets of transform pairs may be defined as follows:

$$g_1(\tau) = \frac{1}{2\pi} \int e^{+i\omega\tau} G_1(\omega)\, d\omega$$

$$G_1(\omega) = \int e^{-i\omega\tau} g_1(\tau)\, d\tau \qquad (2)$$

$$g_2(\tau_1,\tau_2) = \frac{1}{(2\pi)^2} \iint \mathrm{Exp}[+i\omega_1\tau_1 + i\omega_2\tau_2] G_2(\omega_1,\omega_2)\, d\omega_1\, d\omega_2$$

$$G_2(\omega_1,\omega_2) = \iint \mathrm{Exp}[-i\omega_1\tau_1 - i\omega_2\tau_2] g_2(\tau_1,\tau_2)\, d\tau_1\, d\tau_2 \qquad (3)$$

The linear frequency response function, $G_1(\omega)$, defined by Eq. (2) is absolutely conventional. The quadratic frequency response function, $G_2(\omega_1,\omega_2)$ is defined in a <u>bi-frequency</u> plane. Because the kernel $g_2(\tau_1,\tau_2)$ is assumed to be symmetrical in its arguments:

$$g_2(\tau_1,\tau_2) = g_2(\tau_2,\tau_1) \qquad (4)$$

and thus:

$$G_2(\omega_1,\omega_2) = G_2(\omega_2,\omega_1) \qquad (5)$$

$$G_2^*(\omega_1,\omega_2) = G_2(-\omega_1,-\omega_2)$$

$$= G_2(-\omega_2,-\omega_1) \qquad (6)$$

(*The asterisk denotes the complex conjugate.*)

Figure 1a summarizes the results of applying Eq.s (5) and (6) in the bi-frequency plane for the eight possible coordinate positions of two frequencies whose absolute values are a and b. Equation (5) results in a line of symmetry along the line $\omega_2=\omega_1$. Equation (6) results in a line of symmetry of the real part of $G_2(\omega_1,\omega_2)$ defined by $\omega_2=-\omega_1$ (and it may be noted that along this line the imaginary part of the function is zero). These two lines and the ω_1,ω_2 axes divide the bi-frequency plane into octants, of which the two on either side of the positive ω_1 axis may be arbitrarily chosen for reference. The equalities shown in Figure 1a in the remaining six octants are arrived at by applying Eqs. (5) and/or (6). The assumptions of symmetry of the second degree kernel result, with Eq. (3), in a complete definition of $G_2(\omega_1,\omega_2)$ if the functions are defined in any pair of octants including a semi-axis of either frequency. Thus

without loss in generality interpretation of the quadratic frequency response needs only to involve the octants on either side of the positive ω_1 axis. In these octants ω_1 is positive and $|\omega_1| \geq |\omega_2|$.

The interpretation of the quadratic frequency response function is less direct than for the linear case, but can be approached in a similar manner. If in the linear case the system is considered to be excited by

$$\eta(t) = a\cos\omega t$$

the output may then be written:

$$\mathrm{Re}\{aG_1(\omega)\,\mathrm{Exp}(i\omega t)\}$$

and $G_1(\omega)$ is interpreted in terms of normalized amplitude and phase of response.

To interpret the quadratic frequency response, dual harmonic excitation is necessary. Accordingly, it may be assumed that:

$$\eta(t) = a_1\cos\omega_1 t + a_2\cos\omega_2 t \tag{7}$$

In accordance with the previous discussion of symmetry, both frequencies (ω_1, ω_2) are considered positive and $|\omega_1| \geq |\omega_2|$. The basic model, Eq. (1) is good for any zero-mean excitation. Accordingly, Eq. (7) may be substituted directly in Eq. (1). After some algebra the final result for the response to dual harmonic excitation may be written as follows:

$$\begin{aligned}
F_2 = {} & \mathrm{Re}\{a_1 G_1(\omega_1)\,\mathrm{Exp}(i\omega_1 t) + a_2 G_1(\omega_2)\,\mathrm{Exp}(i\omega_2 t)\} \\
& + \frac{1}{2}\{a_1^2 G_2(\omega_1, -\omega_1) + a_2^2 G_2(\omega_2, -\omega_2)\} \\
& + \frac{1}{2}\,\mathrm{Re}\{a_1^2 G_2(\omega_1, \omega_1)\,\mathrm{Exp}(i2\omega_1 t)\} \\
& + \frac{1}{2}\,\mathrm{Re}\{a_2^2 G_2(\omega_2, \omega_2)\,\mathrm{Exp}(i2\omega_2 t)\} \\
& + \mathrm{Re}\{a_1 a_2 G_2(\omega_1, \omega_2)\,\mathrm{Exp}[i(\omega_1+\omega_2)t]\} \\
& + \mathrm{Re}\{a_1 a_2 G_2(\omega_1, -\omega_2)\,\mathrm{Exp}[i(\omega_1-\omega_2)t]\}
\end{aligned} \tag{8}$$

This result shows that the response of the quadratic system, Eq. (1), to dual excitation contains, in general, a shift in the mean and components

of six different frequencies [ω_1, ω_2, $2\omega_1$, $2\omega_2$, $(\omega_1+\omega_2)$, and $(\omega_1-\omega_2)$]. The first two terms of the result are the superposition of the linear responses at the excitation frequencies. The third and fourth terms of Eq. (8) represent a shift in the mean. These terms allow the identification of the mean drifting force or moment operator as the value of $G_2(\omega_1,\omega_2)$ along the line $\omega_2=-\omega_1$ (or $G_2(\omega_1,-\omega_1)$). The fifth and sixth terms are the second harmonic components $(2\omega_1,2\omega_2)$. Similarly, these terms allow the identification of second harmonic response with the values of $G_2(\omega_1,\omega_2)$ along the line $\omega_2=\omega_1$ (or $G_2(\omega_1,\omega_1)$).

The seventh and eighth terms of Eq. (8) pertain to the bi-frequency plane in general. The seventh term is the response at frequency $(\omega_1+\omega_2)$; that is, $G_2(\omega_1,\omega_2)$ expresses the normalized response in the sum frequency due to non-linear interactions. Similarly, the eighth term involves response at frequency $(\omega_1-\omega_2)$; that is, $G_2(\omega_1,-\omega_2)$ is the normalized response in the difference frequency. In terms of Figure 1a, the octant of the bi-frequency plane above the positive ω_1 axis corresponds to the portion of the quadratic frequency response function which defines sum-frequency interactions, and the octant below the positive ω_1 axis corresponds to the portion of the function which defines difference frequency interactions.

Equations (7) and (8) together afford a direct way to proceed in the present investigation. In particular, what is required for a hydromechanical solution for the quadratic frequency response is to solve the hydromechanical problem for <u>dual</u> regular wave excitation.

HYDRODYNAMIC CALCULATIONS

A two-dimensional method for evaluating the lateral second-order force will first be developed and a stripwise calculation of the lateral force and moment in oblique waves will be performed. Thus the formulas of a complete set of quadratic frequency response functions for the lateral drifting force and moment will be obtained.

A. The Lateral Second-Order Force on a Cylinder in Transverse Monochromatic Waves

The second-order lateral forces on a free floating cylinder in regular transverse monochromatic waves will be evaluated at zero forward speed.

The assumptions are that 1) the contribution of the second-order potential to the second-order force is negligibly small when compared to that of the first-order potential, and 2) the drift oscillation is restrained.

The first-order potential which will be used here consists of the sum of the incidence, diffraction and radiation potentials. As is well-known, all the potentials satisfy the linearized boundary conditions at the mean position of oscillations of the body and the free surface as well. Use of such linear potentials and Taylor expansions makes it possible to estimate the second-order force by calculating the contribution of the effect of the instantaneous displacement of the body from its mean position to the resultant time-dependent force.

The body-fixed moving frame is designated by o-yz and the space-fixed frame by O-YZ; the Y-axis rests horizontally on the mean free surface and the Z-axis points vertically upward. Both frames become identical at the mean position of oscillation (Figure 1b).

The instantaneously displaced hull configuration is identified in reference to the fixed frame by using the body coordinates and the motions about its center of gravity.

The motions of the center of gravity of the cylinder consist of sway, heave and roll. The roll-axis passes through the CG as shown in Figure 1b, the coordinates of which are 0, $z-z_o$ where z_o is the vertical coordinate of the center of gravity.

The displacements are designated as

$$S^{(m)}(\omega,t) = \mathrm{Re}\{\bar{S}^{(m)}(\omega)e^{-i\omega t}\} \tag{9}$$

with

$$\bar{S}^{(m)} = S_c^{(m)} + i\, S_s^{(m)} \tag{10}$$

where $m=2,3,4$ indicate sway, heave and roll modes, respectively.

Using the above displacements, the coordinates of a point $A(Y,Z)$ on the body surface at an instantaneous deviated position are calculated by the following equation:

$$\begin{aligned} Y &= S^{(2)} + y\cos S^{(4)} - (z-z_o)\sin S^{(4)} \\ Z &= S^{(3)} + y\sin S^{(4)} + (z-z_o)\cos S^{(4)} \end{aligned} \quad . \tag{11}$$

Expanding $\cos S^{(4)}$ and $\sin S^{(4)}$ in (11) up to the second-order, we have the coordinates (Y and Z) in terms of the displacements and the body coordinates,

$$\begin{aligned} Y &= S^{(2)} + y - (z-z_o)S^{(4)} - \tfrac{1}{2}\, y\, S^{(4)^2} \\ Z &= S^{(3)} + (z-z_o) + y\, S^{(4)} - \tfrac{1}{2}\, S^{(4)^2} \end{aligned} \quad . \tag{12}$$

The above (12) gives the amount of deviation of the point A, i.e., $\{(Y-y),[Z-(z-z_o)]\}$. The corresponding deviation of the velocity potential is approximately estimated by Taylor expansion of the potential at the equilibrium position.

$$\varphi(Y,Z,t) = \varphi(y,z,t) + (Y-y)\varphi_y(y,z,t) + \{Z-(z-z_o)\}\varphi_z(y,z,t) \tag{13}$$

where the $\varphi(y,z,t)$ is the linear velocity potential which has been used in the linear ship motion theory.

Use of the above potential in the Bernoulli pressure equation yields the following expression:

$$\begin{aligned} p(Y,Z,t) = {} & -\rho g Z - \rho\varphi_t(y,z,t) - \rho(Y-y)\varphi_{yt}(x,y,t) - \\ & -\rho\{Z-(z-z_o)\}\varphi_{zt}(y,z,t) - \tfrac{1}{2}\,\rho\{\nabla\varphi(y,z,t)\}^2 \end{aligned} \quad . \tag{14}$$

The integration of the above pressure on the instantaneous body contour

gives the lateral force in the following form:

$$f = \int_{c} p(Y,Z,t)(-dZ) + \int_{c_1} p(Y,Z,t)(-dZ) \tag{15}$$

where $dZ = \sin\alpha\, dS$; dS indicates a segment and α the angle of the segment with respect to the Y-axis. c is the mean wetted contour, whereas c_1 is the deviated instantaneous wetted contour from the mean waterline.[15,16]

Use of Eqs.(12) and (14) in Eq.(15) yields the following second-order lateral force:

$$\begin{aligned} f = {} & \rho g B S^{(3)} S^{(4)} + S^{(4)} \int_{c} \rho\varphi_t \, dy \\ & + \rho \int_{c} \left\{ \left[S^{(2)} - (z - z_o) S^{(4)} \right] \varphi_{yt} + \left[S^{(3)} + y\, S^{(4)} \right] \varphi_{zt} + \frac{1}{2} (\nabla\varphi)^2 \right\} dz \\ & + \rho \int_{c_1} (gZ + \varphi_t)\, dZ \end{aligned} \tag{16}$$

In the above, B indicates the beam of the body, $dy = \cos\alpha\, ds$ and $dz = \sin\alpha\, ds$, where ds indicates a segment on the body contour and α the angle of the segment with the y-axis.

The sum of the first two terms is identical to $\omega^2 m_o S^{(3)}$ where m_o is the mass of the cylinder. This is due to the heaving equation of the cylinder, i.e.,

$$-\omega^2 m_o S^{(3)} = -\rho g B S^{(3)} - \rho \int_{c} \varphi_t dy \quad . \tag{17}$$

where the resultant velocity potential, φ , consists of the radiation potentials due to sway, heave, and roll, and the incident and diffraction potentials. However, the contribution to the integral in Eq.(17) comes from the heave-mode radiation and diffraction potentials due to the symmetry of the body about its vertical axis.

The contour c_1 of the last integral in Eq.(16) consists of the wetted contours on the right and left sides of the hull calculated from the mean waterline. Since $Z + \frac{1}{g}\varphi_t$ is the relative displacement of the hull to the wave elevation, introducing a variable Z_r for the relative wave elevation to the hull displacement, we have the last integral in the form

$$\rho \int_{c_1} (gZ + \varphi_t)\, dZ = -\rho g \int_{c_2} Z_r\, dZ_r$$

where c_2 is the wetted contour for the relative displacement on the right and left sides of the hull, and $dZ_r = dZ = \sin\alpha dS$. Hence,

$$-\rho g \int_{c_2} Z_r dZ_r = -\frac{1}{2}\rho g(r_+^2 - r_-^2) \tag{18}$$

where $r_\pm = e_\pm - (S^{(3)} \pm B/2\ S^{(4)})$ (19)

[the relative wave elevation at the right and left sides of the hull]

$$e_\pm = -\frac{1}{g}\varphi_t(\pm B/2,\ 0,\ t) \tag{20}$$

[the wave elevation at the intersections of the hull and the mean free surface]

Substitution of Eqs.(17) and (18) into (16) yields the second-order lateral force per unit length of the cylinder in the following form:

$$f = \omega^2 m_o S^{(3)} S^{(4)} + \rho \int_c \left\{\left[S^{(2)} - (z-z_o)S^{(4)}\right]\varphi_{yt} + \left[S^{(3)} + yS^{(4)}\right]\varphi_{zt}\right\} dz$$

$$+ \frac{1}{2}\rho \int_c (\nabla\varphi)^2 dz + \frac{1}{2}\rho g(-r_+^2 + r_-^2) \quad . \tag{21}$$

The above Eq.(21) indicates that the second-order lateral force consists of four components. The first is identical to the gyroscopic coupling term between roll and heave motions in the Euler-heave-equation. The second is equal to the sum of two component forces, i.e., the rate of change of the resultant lateral hydrodynamic force per unit lateral displacement times the resultant lateral displacement and the rate of change of the resultant lateral hydrodynamic force per unit vertical displacement times the resultant vertical displacement. The third is the force due to Bernoulli's quadratic pressure. The fourth is due to the relative wave elevation on the hull sidewalls.

The time average of f in Eq.(21) is expected to be nearly identical to Maruo's formula

$$\tilde{f} = \frac{1}{2}\rho g a^2 |\bar{A}_-|^2 \tag{21a}$$

where a is the incident wave amplitude and $\bar{A}_-$ is the vector sum of the wave amplitude ratios due to radiation and diffraction in the far field $Y \to -\infty$.

The present formula has been derived by direct integration of the pressure distribution on the hull surface whereas Maruo's Eq.(21a) is due to the integration of the pressure in the far field. The formula (21), the near-field solution, has an advantage for a clear analysis of the second-order

force, though it does appear to be complicated. It serves also for the evaluation of the quadratic frequency response function for the lateral drifting force and moment.

B. The Lateral Second-Order Force and Moment of a Ship in Oblique Monochromatic Waves

The second-order lateral force and moment of a ship at zero speed in oblique monochromatic waves are evaluated by a stripwise integration of the section force f in Eq.(21).

The oblique wave h is given in the body coordinate system in the following form

$$h = a \cos(\nu x \cos\mu + \nu y \sin\mu - \omega t) \tag{22}$$

where

a = wave amplitude

$\nu = \omega^2/g$ = wave number

μ = angle of incidence (zero in the following wave and $\pi/2$ in the beam wave

The linear response motions $s^{(m)}$ of the ship are determined by solving the coupled heaving-pitching and swaying-rolling-yawing equations. They are denoted by

$$s^{(m)} = \mathrm{Re}\ \bar{s}^{(m)}(\omega) e^{-i\omega t}$$

$$\bar{s}^{(m)} = s_c^{(m)} + i s_s^{(m)} \tag{23}$$

with m=2,3,4,5,6 (= sway, heave, roll, pitch, and yaw, respectively).

Then Eq.(21) gives the lateral second-order force $f(x)$ per unit length of a section at $x=x$ in the following form

$$\begin{aligned} f(x) = {} & \omega^2 m_o(x)\ s^{(3)}(x,\omega)\ s^{(4)}(\omega) \\ & + \rho \int_{c(x)} \left[s^{(2)}(x,\omega) - (z-z_o)\ s^{(4)}(\omega) \right] \varphi_{yt}(\omega)\, dz \\ & + \rho \int_{c(x)} \left[s^{(3)}(x,\omega) + y s^{(4)}(\omega) \right] \varphi_{zt}(\omega)\, dz + \frac{\rho}{2} \int_{c(x)} \left[\nabla\varphi(\omega) \right]^2 dz \\ & + \frac{1}{2} \rho g \left[-r_+^2(x,\omega) + r_-^2(x,\omega) \right] \end{aligned} \tag{24}$$

with

$$S^{(3)}(x,\omega) = S^{(3)}(\omega) - x\, S^{(5)}(\omega)$$

$$S^{(2)}(x,\omega) = S^{(2)}(\omega) + x\, S^{(6)}(\omega) \quad . \tag{25}$$

Integration of the above sectional force over the hull length L yields the resultant force and moment in the following non-dimensional forms:

$$C_F = \frac{1}{\frac{1}{2}\rho g a^2 L} \int_L f(x)\,dx$$

$$= \frac{1}{\frac{1}{2}\rho g L}\left\{ \frac{S^{(4)}(\omega)}{a} \int_L \omega^2 m_o(x) \frac{S^{(3)}(x,\omega)}{a}\,dx \right.$$

$$+ \int_L dx \frac{S^{(2)}(x,\omega)}{a} \int_{c(x)} \rho \frac{\varphi_{yt}(\omega)}{a}\,dz - \frac{S^{(4)}(\omega)}{a} \int_L dx \int_{c(x)} (z-z_o)\rho \frac{\varphi_{yt}(\omega)}{a}\,dz$$

$$+ \int_L dx \frac{S^{(3)}(x,\omega)}{a} \int_{c(x)} \rho \frac{\varphi_{zt}(\omega)}{a}\,dz + \frac{S^{(4)}(\omega)}{a} \int_L dx \int_{c(x)} y\rho \frac{\varphi_{zt}(\omega)}{a}\,dz$$

$$\left. + \frac{1}{2}\rho \int_L dx \int_{c(x)} \left[\frac{\nabla\varphi(\omega)}{a}\right]^2 dz + \frac{1}{2}\rho g \int_L dx \left[-\left(\frac{r_+(x,\omega)}{a}\right)^2 + \left(\frac{r_-(x,\omega)}{a}\right)^2\right]\right\} \tag{26}$$

$$C_M = \frac{1}{\frac{1}{2}\rho g a^2 L^2} \int_L x f(x)\,dx$$

$$= \frac{1}{\frac{1}{2}\rho g L^2}\left\{ \frac{S^{(4)}(\omega)}{a} \int_L \omega^2 m_o(x)\, x \frac{S^{(3)}(x,\omega)}{a}\,dx \right.$$

$$+ \int_L dx\, x \frac{S^{(2)}(x,\omega)}{a} \int_{c(x)} \rho \frac{\varphi_{yt}(\omega)}{a}\,dz - \frac{S^{(4)}(\omega)}{a} \int_L dx\, x \int_{c(x)} (z-z_o)\rho \frac{\varphi_{yt}(\omega)}{a}\,dz$$

$$+ \int_L dx\, x \frac{S^{(3)}(x,\omega)}{a} \int_{c(x)} \rho \frac{\varphi_{zt}(\omega)}{a}\,dz + \frac{S^{(4)}(\omega)}{a} \int_L dx\, x \int_{c(x)} y\rho \frac{\varphi_{zt}(\omega)}{a}\,dz$$

$$\left. + \frac{1}{2}\rho \int_L dx\, x \int_{c(x)} \left[\frac{\nabla\varphi(\omega)}{a}\right]^2 dz + \frac{1}{2}\rho g \int_L dx\, x \left[-\left(\frac{r_+(x,\omega)}{a}\right)^2 + \left(\frac{r_-(x,\omega)}{a}\right)^2\right]\right\} \quad . \tag{27}$$

C. The Quadratic Frequency Response Function for the Lateral Drifting Force and Moment in Dual Oblique Waves

The dual wave is defined by the sum of two monochromatic incident waves (Eq.22)

$$h = \sum_{n=1,2} a_n \cos[\nu_n x \cos\mu + \nu_n y \sin\mu - \omega_n t] \quad . \tag{28}$$

The corresponding dual response motion and potential are also defined by the sums of the response to each monochromatic wave, such as

$$\sum_{n=1,2} S^{(m)}(\omega_n) \quad \text{and} \quad \sum_{n=1,2} \varphi_t(\omega_n) \quad . \tag{28a}$$

Substitution of the above dual harmonic into Eqs.(26) and (27) yields the quadratic frequency response functions for the lateral drifting force and moment in dual oblique waves in the following non-dimensional form:

$$\begin{aligned} C_F = \frac{1}{\frac{1}{2}\rho g L} \Bigg\{ & \sum_{m=1,2} \frac{S^{(4)}(\omega_m)}{a_m} \int_L \omega_n^2 m_o(x) \sum_{n=1,2} \frac{S^{(3)}(x,\omega_n)}{a_n} dx \\ & + \int_L dx \sum_{m=1,2} \frac{S^{(2)}(x,\omega_m)}{a_m} \int_{c(x)} \sum_{n=1,2} \frac{\varphi_{yt}(\omega_n)}{a_n} dz \\ & - \sum_{m=1,2} \frac{S^{(4)}(\omega_m)}{a_m} \int_L dx \int_{c(x)} (z-z_o) \sum_{n=1,2} \frac{\varphi_{yt}(\omega_n)}{a_n} dz \\ & + \int_L dx \sum_{m=1,2} \frac{S^{(3)}(x,\omega_m)}{a_m} \int_{c(x)} \sum_{n=1,2} \frac{\varphi_{zt}(\omega_n)}{a_n} dz \\ & + \sum_{m=1,2} \frac{S^{(4)}(\omega_m)}{a_m} \int_L dx \int_{c(x)} y \sum_{n=1,2} \frac{\varphi_{zt}(\omega_n)}{a_n} dz \\ & + \frac{\rho}{2} \int_L dx \int_{c(x)} \sum_{m=1,2} \frac{\nabla\varphi(\omega_m)}{a_m} \sum_{n=1,2} \frac{\nabla\varphi(\omega_n)}{a_n} dz \\ & + \frac{\rho g}{2} \int_L dx \left\{ - \sum_{m=1,2} \frac{r_+(\omega_m)}{a_m} \sum_{n=1,2} \frac{r_+(\omega_n)}{a_n} + \sum_{m=1,2} \frac{r_-(\omega_m)}{a_m} \sum_{n=1,2} \frac{r_-(\omega_n)}{a_n} \right\} \Bigg\} \quad . \end{aligned} \tag{29}$$

$$C_M = \frac{1}{\frac{1}{2}\rho g L^2}\Bigg\{ \sum_{m=1,2} \frac{S^{(4)}(\omega_m)}{a_m} \int_L \omega_n^2 m_o(x)\, x \sum_{n=1,2} \frac{S^{(3)}(x,\omega_n)}{a_n}\, dx$$

$$+ \int_L dx \times \sum_{m=1,2} \frac{S^{(2)}(x,\omega_m)}{a_m} \int_{c(x)} \rho \sum_{n=1,2} \frac{\varphi_{yt}(\omega_n)}{a_n}\, dz$$

$$- \sum_{m=1,2} \frac{S^{(4)}(\omega_m)}{a_m} \int_L dx \times \int_{c(x)} (z-z_o)\, \rho \sum_{n=1,2} \frac{\varphi_{yt}(\omega_n)}{a_n}\, dz$$

$$+ \int_L dx \times \sum_{m=1,2} \frac{S^{(3)}(x,\omega_m)}{a_m} \int_{c(x)} \sum_{n=1,2} \frac{\varphi_{zt}(\omega_n)}{a_n}\, dz$$

$$+ \sum_{m=1,2} \frac{S^{(4)}(\omega_m)}{a_m} \int_L dx \times \int_{c(x)} y\, \rho \sum_{n=1,2} \frac{\varphi_{zt}(\omega_n)}{a_n}\, dz$$

$$+ \frac{1}{2}\rho \int_L dx \times \int_{c(x)} \sum_{m=1,2} \frac{\nabla\varphi(\omega_m)}{a_m} \sum_{n=1,2} \frac{\nabla\varphi(\omega_n)}{a_n}\, dz$$

$$+ \frac{1}{2}\rho g \int_L dx \times \left\{ - \sum_{m=1,2} \frac{r_+(\omega_m)}{a_m} \sum_{n=1,2} \frac{r_-(\omega_n)}{a_n} + \sum_{m=1,2} \frac{r_-(\omega_m)}{a_m} \sum_{n=1,2} \frac{r_+(\omega_n)}{a_n} \right\} \Bigg\} . \tag{30}$$

Equation (29) or (30) consists of seven terms, each of which with omission of $\frac{1}{2}\rho g L$ or $\frac{1}{2}\rho g L^2$ is expressed in the following form:

$$I_k = \mathrm{Re}\left\{ \sum_{m=1,2} \bar{A}_k(\omega_m) e^{-i\omega_m t} \right\} \mathrm{Re}\left\{ \sum_{n=1,2} \bar{B}_k(\omega_n) e^{-i\omega_n t} \right\} \tag{31}$$

where $\bar{A}_k, \bar{B}_k$ = complex frequency response amplitudes.

For the analysis of the quadratic frequency response function, one defines a fundamental function $H_{1,k}$ for each I_k in the form

$$H_{1,k}(\omega_m,\omega_n) = \bar{A}_k(\omega_m)\bar{B}_k(\omega_n)$$

$$H_{1,k}(\omega_m,-\omega_n) = \bar{A}_k(\omega_m)\bar{B}_k^*(\omega_n)$$

$$H_{1,k}^*(\omega_m,-\omega_n) = H_{1,k}(-\omega_m,\omega_n) \tag{32}$$

where the asterisk indicates the complex conjugate of the function.

Use of the above functions for the k^{th} term of Eqs.(29) or (30) yields the following expression:

$$
\begin{aligned}
I_k = \frac{1}{2}\Big\{ & \mathrm{Re}\left[H_{1,k}(\omega_m,-\omega_m) + H_{1,k}(\omega_n,-\omega_n)\right] \\
& + \mathrm{Re}\left[H_{1,k}(\omega_m,\omega_m)e^{-i2\omega_m t}\right] \\
& + \mathrm{Re}\left[H_{1,k}(\omega_n,\omega_n)e^{-i2\omega_n t}\right] \\
& + \mathrm{Re}\left[\left[H_{1,k}(\omega_m,\omega_n) + H_{1,k}(\omega_n,\omega_m)\right]e^{-i(\omega_m+\omega_n)t}\right] \\
& + \mathrm{Re}\left[\left[H_{1,k}(\omega_m,-\omega_n) + H^{*}_{1,k}(\omega_n,-\omega_m)\right]e^{-i(\omega_m-\omega_n)t}\right]\Big\} \quad . \qquad (33)
\end{aligned}
$$

Now one defines the quadratic frequency response function $G_2(\omega_m,\omega_n)$:

$$
\begin{aligned}
G_2(\omega_m,\omega_n) &= \frac{1}{2}\sum_{k=1}^{7}\left[H_{1,k}(\omega_m,\omega_n) + H_{1,k}(\omega_n,\omega_m)\right] \\
G_2(\omega_m,-\omega_n) &= \frac{1}{2}\sum_{k=1}^{7}\left[H_{1,k}(\omega_m,-\omega_n) + H^{*}_{1,k}(\omega_n,-\omega_m)\right] \quad . \qquad (34)
\end{aligned}
$$

Use of the definitions (Eq.32) makes the $G_2(\omega_m,\omega_n)$ in Eqs.(34) satisfy the symmetry relationships previously indicated in Eqs.(5) and (6).

Thus the non-dimensional drifting force C_F (Eq.29) and moment C_M (Eq.30) are expressed in terms of the quadratic frequency response function G_2 (Eq.34) in the following form:

$$
\begin{aligned}
\begin{Bmatrix} C_F \\ C_M \end{Bmatrix} = \begin{Bmatrix} \frac{1}{\frac{1}{2}\rho g L} \\ \frac{1}{\frac{1}{2}\rho g L^2} \end{Bmatrix} \Big\{ & \frac{1}{2}\left\{G_2(\omega_{ih},-\omega_{ih}) + G_2(\omega_n,-\omega_n)\right\} \\
& + \frac{1}{2}\,\mathrm{Re}\left\{G_2(\omega_m,\omega_m)e^{-i2\omega_m t}\right\} \\
& + \frac{1}{2}\,\mathrm{Re}\left\{G_2(\omega_n,\omega_n)e^{-i2\omega_n t}\right\} \\
& + \mathrm{Re}\left\{G_2(\omega_m,\omega_n)e^{-i(\omega_m+\omega_n)t}\right\} \\
& + \mathrm{Re}\left\{G_2(\omega_m,-\omega_n)e^{-i(\omega_m-\omega_n)t}\right\}\Big\} \quad . \qquad (35)
\end{aligned}
$$

where the G_2 represents the quadratic frequency response function for the lateral drifting force or moment.

In dimensional form, they are given by

$$\left.\begin{matrix} F \\ M \end{matrix}\right\} = \frac{1}{2}\left\{a_m^2 G_2(\omega_m,-\omega_m) + a_n^2 G_2(\omega_n,-\omega_n)\right\}$$

$$+ \frac{1}{2}\,\mathrm{Re}\left\{a_m^2 G_2(\omega_m,\omega_m)e^{-i2\omega_m t}\right\}$$

$$+ \frac{1}{2}\,\mathrm{Re}\left\{a_n^2 G_2(\omega_n,\omega_n)e^{-i2\omega_n t}\right\}$$

$$+ \mathrm{Re}\left\{a_m a_n G_2(\omega_m,\omega_n)e^{-i(\omega_m+\omega_n)t}\right\}$$

$$+ \mathrm{Re}\left\{a_m a_n G_2(\omega_m,-\omega_n)e^{-i(\omega_m-\omega_n)t}\right\} \quad . \tag{36}$$

The mean drifting force and moment deduced from Eq.(35) are given by

$$\left\{\begin{matrix} \bar{C}_F \\ \bar{C}_M \end{matrix}\right\} = \left\{\begin{matrix} \frac{1}{\rho g L} \\ \frac{1}{\rho g L^2} \end{matrix}\right\} G_2(\omega_m,-\omega_m) \tag{37}$$

where suffixes F and M indicate the G_2 for force and moment, respectively.

D. Calculation of the $H_{1,k}$ Function

The $H_{1,k}$ functions which have been defined in Eq.(32) are evaluated in Appendices A, B, C, and D.

The $H_{1,k}$ functions for the drifting force are shown in Appendix A whereas those for the drifting moment are in Appendix B.

The resultant velocity potential, hydrodynamic pressure and velocity components are evaluated in Appendix C.

Formulas in Appendices A and B contain the terms of hydrodynamic pressures and velocity components. These are evaluated in Appendix C.

The resultant velocity potential (Eq.C-15) is utilized in calculating the hydrodynamic pressure (Eq.C-16 to Eq.C-18) and the velocity components (Eq.C-19). It is also used in the evaluation of the diffracted and radiated wave amplitudes in the far-field which serve for the evaluation of Maruo's formula (21a). The asymptotic expression of the potential in the far field is given in the Appendix of Reference 11.

The velocity components due to radiation and diffraction are calculated by using the formulas for the unit source-induced velocity components, which are given in Appendix D.

NUMERICAL CALCULATIONS

A. Comparison of Analytical and Experimental Estimates of the Mean Drifting Force and Moment

The previously defined non-dimensional mean drifting force and moment coefficients $\bar{C}_F + \bar{C}_M$ (Eq.37) are the values of the quadratic frequency response functions along the line $\omega_m = -\omega_n$, and it is this particular section of the functions for which there are a number of confirming data.

The models chosen for the comparisons are 1) the cylinder tested by Koterayama,[17] and 2) the Series 60, 0.60 C_B parent which was used by Lalangas.[12] The principal particulars of the models are given in Tables 1 and 2.

The non-dimensional coefficients $\bar{C}_F$ and $\bar{C}_M$ (Eq.37) are expressed in terms of the previously defined $H_{1,k}$ functions (Appendices A and B), each of which consists of four components as shown below:

$$\bar{C}_F = \sum_{n=1,4} \bar{C}_{Fn}$$

$$\bar{C}_M = \sum_{n=1,4} \bar{C}_{Mn} \tag{38}$$

with

$$\left.\begin{matrix} \bar{C}_{F_1} \\ \bar{C}_{M_1} \end{matrix}\right\} = \begin{matrix} \frac{1}{\rho g L} \ \mathrm{Re}\ H^F_{1,1}(\omega,-\omega) \\ \frac{1}{\rho g L^2} \ \mathrm{Re}\ H^M_{1,1}(\omega,-\omega) \end{matrix} \tag{39a}$$

$$\left.\begin{matrix} \bar{C}_{F_2} \\ \bar{C}_{M_2} \end{matrix}\right\} = \begin{matrix} \frac{1}{\rho g L} \ \mathrm{Re} \sum_{\ell=2}^{5} H^F_{1,\ell}(\omega,-\omega) \\ \frac{1}{\rho g L^2} \ \mathrm{Re} \sum_{\ell=2}^{5} H^M_{1,\ell}(\omega,-\omega) \end{matrix} \tag{39b}$$

$$\begin{matrix} \bar{C}_{F_3} \\ \bar{C}_{M_3} \end{matrix} = \begin{matrix} \frac{1}{\rho g L} \\ \frac{1}{\rho g L^2} \end{matrix} \text{Re } H^{\begin{matrix} F \\ M \end{matrix}}_{1,6}(\omega, -\omega) \tag{39c}$$

$$\begin{matrix} \bar{C}_{F_4} \\ \bar{C}_{M_4} \end{matrix} = \begin{matrix} \frac{1}{\rho g L} \\ \frac{1}{\rho g L^2} \end{matrix} \text{Re } H^{\begin{matrix} F \\ M \end{matrix}}_{1,7}(\omega, -\omega) \tag{39d}$$

where superscripts F and M to the $H_{1,k}$ indicate the functions for drifting force and moment, respectively.

The first coefficients (Eqs. 39a, A-4, B-4) are known as the gyroscopic coupling terms in Euler's equation for a body moving in a vacuum.[21] Vossers gives a discussion of the $\bar{C}_{M_1}$ describing its influence on the steering of a ship.

Equation (39b) is the sum of two, i.e., a) the product of [the rate of change of the resultant lateral hydrodynamic force (moment)] and [the resultant lateral displacement], and b) the product of [the rate of change of the resultant vertical hydrodynamic force (moment)] and [the resultant vertical displacement].

The third terms are due to the Bernoulli quadratic hydrodynamic pressure. It is to be noted that Bernoulli's mean second-order force and moment appear as one of the four components of the total drifting force or moment.

The fourth coefficients are due to the relative wave elevation along the intersection of the mean free surface and hull surface at its mean position.

According to the aforementioned remarks, the four components may be designated as: 1) the gyroscopic coupling, 2) the force (moment) rate x displacement, 3) the Bernoulli quadratic, and 4) the relative wave components.

Cylinder:

The four components $\bar{C}_{F_m}$ of the mean drifting force coefficients on the cylinder[17] versus the non-dimensional wave frequency parameter $\nu B/2$ are shown in Figure 2a. Two arrows pointing downward indicate the resonance frequencies of roll and heave. All the components indicate peaks at the roll resonance frequency. The second peaks of the components corresponding to the heave resonance fall slightly apart from the resonance frequency. However, the peaks of the gyroscopic-coupling and the force rate x displacement terms fall nearer to the resonance frequency than the others. This is attributed to the fact that the former terms are more sensitive to the response motions than the latter. The influence of the resonance motions on the relative wave component is illustrated in Figure 2b.

The gyroscopic-coupling term $\bar{C}_{F_1}$ is negative all along the frequency axis. This is due to the fact that for the model the phase differences between the rolling and heaving displacements are greater than $\pi/2$ in the entire frequency domain.

The force rate x displacement term indicates its peak at roll resonance and negative peak in response to heave resonance.

The Bernoulli quadratic component appears to be negative in the entire frequency domain, which results from the force unbalance due to the quadratic pressure asymmetric with respect to the vertical z-axis.

The relative wave term $\bar{C}_{F_4}$ is dominant among the components. It exceeds and counteracts all the rest of the components and thus yields the positive resultant drifting force, which remains below unity. This confirms the calculation and agrees with the energy conservation law. The behavior of the magnitudes of the ratio of relative elevation to incident wave amplitude $|r_{\pm}/a|$ is illustrated in Figure 2b, where $\pm$ indicate the locations, i.e., the intersections of the hull surfaces at equilibrium with the mean free surfaces along the positive and negative y-axis. When the body is free, it is evidently affected by the resonance motions.

The asymptotic behavior of the force components for the infinite frequency are estimated as follows:

As the frequency approaches infinity, the response motion vanishes and it results that 1) the hull motion dependent gyroscopic-coupling and force rate x displacement terms will vanish, and 2) the relative wave elevations for

free body reach to the state of perfect reflection against a fixed body. In mathematical form we have

$$\left.\begin{matrix}\bar{C}_{F_1}\\ \bar{C}_{F_2}\end{matrix}\right\} \to 0 \qquad \text{(40a)}$$

$$\text{frequency} \to \infty \quad ,$$

and

$$|r_-| \to 2a$$
$$|r_+| \to 0 \quad . \qquad \text{(40b)}$$

Hence, referring to (39d) and (A-28),

$$\bar{C}_{F_4} \to 2.0 \quad . \qquad \text{(40c)}$$

According to the energy conservation in perfect reflection at infinite frequency. we have

$$\bar{C}_F \to 1.0 \quad . \qquad \text{(40d)}$$

Thus, it is inferred that

$$\bar{C}_{F_3} \to -1.0 \quad . \qquad \text{(40e)}$$

For the vanishingly low frequency, the four components are estimated in the following manner:

The phase difference between heave and roll is $\pi/2$ in Eq.(A-4), thus $\bar{C}_{F_1} \to 0$; since the hydrodynamic force rate is linearly proportional to the wave frequency (Eq.A-6), $\bar{C}_{F_2} \to 0$. Since the heave phase is zero and roll phase is $\pi/2$, the components $S_s^{(3)}$ and $S_c^{(4)}$ vanish together with the terms containing ω in Eq.(A-30). Thus due to (A-28), $\bar{C}_{F_4} \to 0$. Since the transmission of energy is perfect, $\bar{C}_F \to 0$. Hence it is inferred that the Bernoulli quadratic term $\bar{C}_{F_3} \to 0$.

Figure 2c illustrates a comparison of the analytical methods and experimental values. Maruo's far-field theory is presented by a dotted line and the present near-field method is indicated by a solid line. Both results are in good agreement as was expected. The near-field value indicates the effect

of roll resonance, whereas the far-field procedure does not. The experimental values indicate higher values than unity in the high frequency region.

Ship:

The four constituents of the beam sea mean drifting force acting on the ship, Reference 12, are illustrated in Figure 3a in coefficient form. The behavior of the following coefficients appear to be similar to that of the cylinder in that 1) the hull-motion dependent terms $\bar{C}_{F_1}$ and $\bar{C}_{F_2}$ show their peaks at (or near) the heave resonance frequency (see Figure 3b); 2) the phase difference between heave and roll as shown in Figure 3b appears to be greater than $\pi/2$, resulting in a negative gyroscopic-coupling term; and 3) the relative wave and Bernoulli's quadratic terms reach to their peaks in the neighborhood of the heave resonance.

The resultant mean drifting forces and moments are illustrated in Figure 3c. Maruo's method and experimental model data are compared with the results of the present calculation. The comparison shows excellent agreement in beam seas. In oblique seas, the two analytical methods are in good agreement, as shown in Figures 3d and 3e.

The Irregular Frequency Phenomenon:

The presence of a mathematical discontinuity in the mean drifting force at $\nu B/2 \approx 1.87$ for the cylinder has been investigated. The discontinuity is due to the eigenfrequency of the fluid motion inside the hull. Referring to the work of Ogilvie and Shin,[18] a modification of the Green's function has been performed just for the heave mode since its contribution is regarded dominant. After a trial-and-error study, we have selected the constant C of 0.033.

Figure 4 illustrates that the modification is virtually effective in reducing the discontinuity behavior of the drifting force.

B. The Quadratic Frequency Response Function for Lateral Force

The purpose of the development of computational methods for quadratic response functions is to enable improvement in the capability of predicting the non-linear lateral force and moments induced by irregular waves. In practical terms, the important part of the sway/yaw/surge response of ships is not the part which may be predicted by linear methods, but the low-frequency non-linear part; that is, the forces which occur at frequencies below the lowest wave excitation frequencies of significance. Given the quadratic frequency response function and a specification of the irregular waves, the contribution to lateral forces of the quadratic non-linearities treated herein may be computed either in the time or frequency domain.[2] Insofar as engineering predictions are concerned, it appears reasonable to consider the predicted very low frequency forces as excitation to a linearized representation of sway and yaw (as in Reference 3) so that analytical prediction of the important features of the non-restored modes of motion in irregular seas is within reach - to the extent of course that the estimated quadratic frequency response functions are valid.

The portions of the quadratic frequency response function pertaining to interactions between two different frequencies are of importance in the above respect. Since the preceding sections of the report have indicated some quite favorable experimental/analytical comparisons for the mean drift and moment function ($G_2(\omega,-\omega)$), the next logical step would be to compare analysis and experiment for the general function ($G_2(\omega_1,\omega_2)$), (or, at least parts of it). Because no suitable experiments had been conducted as of the time of writing, this next logical step was not possible. Thus the most that was reasonable to do in this circumstance was to compute a typical quadratic response function for assumed experimental conditions, and to examine its plausability relative to previous experience.

To this end the model ship (Series 60, C_B=0.6) as used in Reference 12, and for which the mean drift force response was considered earlier, was assumed to be at a sixty-degree heading to waves, at zero speed, and the computations indicated in Eqs.(29, (31), (32), and (34) were carried out for the lateral drift force components. The values of the function were non-dimensionalized in the form implied by Eq.(37); that is, the dimensional values of (force)/length)^2 were divided by ρgL. It was convenient to non-dimensionalize

the frequencies in the following form:

$$\sigma_m = \omega_n/\omega_{1L} \qquad (= \sqrt{L/\lambda})$$

where:

$$\omega_{1L} = \sqrt{2\pi g/L}$$

L = ship length

λ = wave length

The computation was carried out for all combinations of a non-dimensional input frequency range from σ=0.373 to 2.2 ($\lambda/L \cong 0.2$ to 7.2). Thirty equally spaced frequency steps were utilized within this range to reasonably define the function.

In order to visualize the results it is advantageous to utilize the planes of symmetry discussed in conjunction with Figure 1a, and thus also of advantage to introduce the frequency transformation of Reference 2. This transformation maps the ω_1, ω_2 plane (see Figure1a) into a sum and difference frequency plane in accordance with

$$\Omega_1 = \omega_1 - \omega_2 = \text{difference frequency}$$

$$\Omega_2 = \omega_1 + \omega_2 = \text{sum frequency} \qquad (41)$$

The Ω_1, Ω_2 plane is shown mapped into the ω_1, ω_2 plane in Figure 5. The Ω_1, Ω_2 axes are coincident with the lines of symmetry noted in the discussion of Figure 1a. In accordance with the discussion of Figure 1a, the fundamental symmetry of the quadratic frequency response function allows complete definition if the function is known in a quadrant of the plane defined by the lines of symmetry. The quadrant of the Ω_1, Ω_2 plane (Figure 5) in which both sum and difference frequencies are positive corresponds to the quadrant selected earlier in interpreting the response to dual harmonic excitation. Also in accordance with the earlier discussion of dual harmonic excitation, the sum frequency, Ω_2, corresponds and is numerically equal to, the output frequency. Any combination of input frequencies ω_1 and ω_2 which are on the line Ω_2 = constant will generate a component at that frequency. For example, the mean drift force operator involves output frequency of zero and is located on the Ω_1 axis. The frequency transformation involves no distortion of the magnitude

of the quadratic frequency response function, merely providing a somewhat more convenient way of looking at it. Since the non-dimensional frequencies (σ_n) differ from the dimensional frequencies (ω_n) only by a scale factor, σ_1 and σ_2 may be substituted for ω_1 and ω_2 in Eq.(41) and the resulting Ω_1, Ω_2 system taken to be non-dimensional.

Figure 6 is an isometric plot of the modulus of the analytically determined quadratic frequency response function. The "view" is toward the origin of the bi-frequency plane from a position above the ω_1 axis (Figure 5). (The difference frequency axis (Ω_1) is to the left, the sum frequency axis is to the right, and the modulus of the function is "vertical".) The lines defining the function contours are in the nature of section lines which are parallel to the Ω_1 and Ω_2 axes. Each intersection corresponds to an analytically computed point, and the connecting line segments are straight. There were actually about twice as many points computed as are shown. In the figure the plotted domain of the bi-frequency plane appears triangular. This is the result of computing the function to a maximum absolute input frequency of 2.2. The right-to-left section at the front of the plot is indicated with vertical lines defining the position of computed points. This section represents the modulus of the function along the line $\sigma_1 = 2.2$. There is an exactly flat portion shown in the center of the surface because, as an economy measure, no computations were carried out for input frequencies between 0 and 0.373, and for plotting purposes the magnitude of the interactions between these frequencies and all others was assumed to be zero.

Figure 7 has been prepared as an aid to discussion, as well as to round out the presentation in Figure 6. At the bottom of this figure the linear roll and heave responses are shown in non-dimensional form plotted on input frequency, σ. The lower two frames of the figure indicate the modulus of the quadratic frequency response function on the lines of symmetry; that is, along the lines $\Omega_1 = 0$ and $\Omega_2 = 0$. In these special cases there is a one-to-one correspondence between input frequency and the sum and difference frequencies Ω_1 and Ω_2 since the function may in these cases be considered to indicate the mean shift and second harmonic response for excitation at a single frequency.

Qualitatively, Figures 6 and 7 show that the modulus of the computed quadratic frequency response function resembles that which is expected from previous work with added resistance (Reference 1). There are two main humps

shown within the range of computation, one associated with difference frequency interactions, one associated with sum-frequency interactions, and the two humps are not symmetrical.

Several more detailed observations can be made. As was noted in the presentation of Figure 6, the apparent flat valley in the middle comes about because no computations were made. The edge of this valley has some minor "cliffs" which (translated into the σ_1 σ_2 plane) occur along the lines $\sigma_2 \equiv \pm 0.4$ for σ_1 greater than about 1. This means simply that the interactions of long low frequency waves with much shorter high frequency waves are a good deal larger than the value of the quadratic frequency response function in the planes of symmetry would lead one to expect. Comparing Figures 6 and 7, the most important magnitudes of the function occur near heave resonance so that it appears that non-linear interactions between very long waves and waves causing heave resonance can be non-negligible, though of secondary magnitude.

The next observation from Figure 6 is that there appears to be two chains of secondary (and not well resolved) peaks in the modulus of the function running parallel to the "cliffs" just mentioned. Comparing the frequencies in Figure 7 it is clear that these peaks are the result of resonant rolling. As shown in Figure 7, the computed rolling is lightly damped because the present computation is made for zero ship speed, and low "viscous" roll damping effects have been assumed. Rolling is thus shown to have a secondary, though possibly not entirely negligible effect on the lateral drift force function since the computations show interactions between responses at roll resonance and at frequencies approaching heave resonance to be relatively larger than the mean drift response near roll resonance shown in Figure 7.

The most important practical part of the function in Figure 6 is that to the left, the part which influences low frequency response, and this part of the function appears smooth and relatively uncomplicated. There is a notch in the mean operator, Figure 7, at a frequency of $\sigma \cong 2.1$ ($\Omega_1 \cong 4.2$), and this is traceable to an "irregular" frequency. As noted in the previous section, the technique adopted for minimizing the effects of irregular frequencies does not completely eliminate the problem. Effects of this irregular frequency are included in some way for all estimates of the quadratic frequency response function involving input frequency of $\sigma = 2.1$. The largest input

frequency for which computations were made ($\sigma = 2.2$) corresponds to (wave length)/ship length of 0.2. As far as showing a picture of the complete function this is too long a wave length, but any wave length would be too long since it was shown that the mean drift force operator is asymptotic to a constant as wave length goes toward zero. It can only be surmised, but it appears that the quadratic frequency response function continues indefinitely along the Ω_1 axis about as shown in Figure 6 for the highest frequencies computed. This last feature of the function complicates, but does not prevent, practical predictions for irregular waves[2] since the magnitudes of very-very short waves in an irregular sea are ordinarily extremely small relative to the magnitudes of waves near ship length and longer.

The last feature of the computed quadratic frequency response function, the most significant part of the sum-frequency interactions (to the right in Figure 6), is the one that the least is known about. The computed peak modulus for second harmonic response (Figure 7) is about twice that for the mean drift force response and has a hump and hollow. Why these come about is not immediately obvious. It is again a surmise, but if the difference frequency part of the function continues indefinitely along the Ω_1 axis, significant values of the sum-frequency part would be expected to continue indefinitely along the Ω_2 axis. The range of the computation is too short to convincingly demonstrate the behavior of the function in this direction.

CONCLUSIONS AND RECOMMENDATIONS

What has been accomplished thus far is the development of a "near field", second-order strip theory for lateral force and moment on a ship at zero speed which is, moreover, formulated in such a way that the results of the hydromechanical analyses may be immediately connected with a long existing general input/output theory for weakly non-linear systems. As a result of the formulation the computation of all the quadratic, non-linear interaction responses between pairs of waves (the "complete" quadratic frequency response function) is hardly more expensive than a careful linear motions analysis utilizing the strip "close-fit" approach.

To the extent that the results of the present development can be compared with experiment, the comparision appears favorable. However, the experimental data available are concerned only with some very special values of the quadratic frequency response function (in fact, values of the mean drifting force and moment measured in monochromatic waves). Thus while the present analysis is capable of predicting what appears to be a plausible complete quadratic frequency response function, experimental confirmation, either direct or indirect, of the entire computation is lacking.

In order to make further progress in this area some experiments, which go beyond the conventional, need to be carried out, with the objectives: a) of enabling comparisons of experiment and theory in at least the most important areas of the bi-frequency domain, and b) of enabling comparisons to be made between lateral drifting forces and moments in irregular seas and those predicted completely by analytical methods.

Since the influence of the quadratic non-linearities in lateral wave induced forces can be important in applications where precise directional control of ships is required, an extention of the present methods to include forward speed is also recommended.

REFERENCES

1. Dalzell, J.F. and Kim, C.H., "Analytical Investigation of the Quadratic Frequency Response for Added Resistance," Report SIT-DL-76-1878, August 1976.

2. Dalzell, J.F., "The Applicability of the Functional Polynomial Input-Output Model to Ship Resistance in Waves," SIT-DL-75-1794, January 1975.

3. Kim, C.H. and Breslin, J.P., "Prediction of Slow Drift Oscillations of a Moored Ship in Head Seas," Behaviour of Offshore Structures, Proceedings of the First International Conference, Vol. 1; held at the Norwegian Institute of Technology, The University of Trondheim, Norway, August 2, 1976.

4. Hsu, F.H. and Blenkarn, K.A., "Analysis of Peak Mooring Forces Caused by Slow Vessel Drift Oscillations in Random Seas," OTC Paper 1159, Offshore Technology Conference, Houston, 1970.

5. Newman, J.N., "Second Order Slowly Varying Forces on Vessels in Irregular Waves," International Symposium on the Dynamics of Marine Vehicles and Structures in Waves, University College, London, April 1974.

6. Faltinsen, Odd M. and Loken, Arne, "Drift Forces and Slowly-Varying Horizontal Forces on a Ship in Waves," Symp. on Applied Mathematics, dedicated to the late Prof. Dr. R. Timman, Jan.1978, Delft Univ. Press.

7. Maruo, H., "The Drift of a Body Floating on Waves," Journal of Ship Research, Vol.4, No.3, December 1960.

8. Ogawa, A., "The Drifting Force and Moment on a Ship in Oblique Regular Waves," International Shipbuilding Progress, Vol.14, No.149, January 1967.

9. Spens, P.G. and Lalangas, P.A., "Measurements of the Mean Lateral Force and Yawing Moment on a Series 60 Model in Oblique Regular Waves," Davidson Laboratory Report 880, Stevens Institute of Technology, 1962.

10. Newman, J.N. "The Drift Force and Moment on Ships in Waves," Journal of Ship Research, March 1967.

11. Kim, C.H. and Chou, F., "Prediction of Drifting Force and Moment on an Ocean Platform Floating in Oblique Seas," Report SIT-OE-70-2, December 1970; also published in ISP, Vol.20, No.230, October 1973.

12. Lalangas, P., "Lateral and Vertical Forces and Moments on a Restrained Series 60 Ship Model in Oblique Regular Waves," Report 920, Davidson Laboratory, Stevens Institute of Technology, October 1963.

13. Salvesen, N., "Paper 22. Second-Order Steady-State Forces and Moments on Surface Ships in Oblique Regular Waves," International Symposium

on the Dynamics of Marine Vehicles and Structures in Waves, London, April 1974.

14. Pinkster, J.A. and van Oortmerssen, G., "Computation of the First and Second Order Wave Forces on Bodies Oscillating in Regular Waves," Proceedings of the Second International Conference on Numerical Ship Hydrodynamics, University of California, pp.136-156, September 1977.

15. Potash, R.L., "Second Order Theory of Oscillating Cylinders," Journal of Ship Research, Vol.15, No. 4, 1971.

16. Söding, H., "Second Order Forces on Oscillating Cylinders in Waves," Schiffstechnik Bd. 23, 1976.

17. Koterayama, W., "Motions of Moored Floating Body and Tension of Mooring Lines in Waves," Journal of Seibu-Zosen-Kai, November 1976.

18. Ogilvie, T.F. and Shin, Y.S., "Integral-Equations Solutions for Time-Dependent Free-Surface Problems," Journal of the Society of Naval Architects of Japan, Vol.143, June 1978.

19. Liao, Ping, "The Contributions of the First Order Potential to the Second Order Forces," Master's Thesis, Ocean Engineering, Stevens Institute of Technology, May 1977.

20. Frank, W., "On the Oscillation of Cylinders in or Below the Free Surface of Deep Fluids," NSRDC Report 2375, October 1967.

21. Vossers, G., "Resistance, Propulsion and Steering of Ships, C: Behavior of Ships in Waves," Technical Publishing Co., H. Stom N.V. Haarlem (The Netherlands), pp.98-99, 1962.

ACKNOWLEDGMENT

The authors wish to express their appreciation to Mr. Ping Liao for his assistance in the programming of the velocity components due to the unit pulsating source.

TABLE I

PRINCIPAL PARTICULARS

The particulars of Koyerayama's model, which have been used in the present calculation, are tabulated below:

Cylinder Shape of a Lewis-Form Section

Section Area Coefficient (due to close-fit)	0.9326*
Beam, ft	1.64
Draft, ft	0.656
Roll Gyradius, ft	0.5711
Metacentric Height, ft	0.12464
Vertical Center of Gravity (below waterline)	-0.07544**
Roll Period, sec	1.895
Roll Damping Factor	0.62

*original value: 0.942

**original value: -0.108

TABLE 2

MODEL PARTICULARS
Series 60, C_B=0.6

LBP, L, ft	5.00
Breadth, B, ft	0.667
Draft (level trim), T, ft	0.267
Displacement (F.W.), Δ, lb	33.27
LCG (abaft midsection), ft	0.075
VCG (below waterline), $\overline{OG}$, ft	0.022
Rudder area, ft^2	0.030
Waterplane Area, A_w, ft^2	2.355
Load Waterline Coefficient, C_w	0.706
Pitch Gyradius, κ_ψ, ft	1.275
Yaw Gyradius, κ_χ, ft	1.275
Roll Metacentric Height, $\overline{GM}_\varphi$, ft	0.025

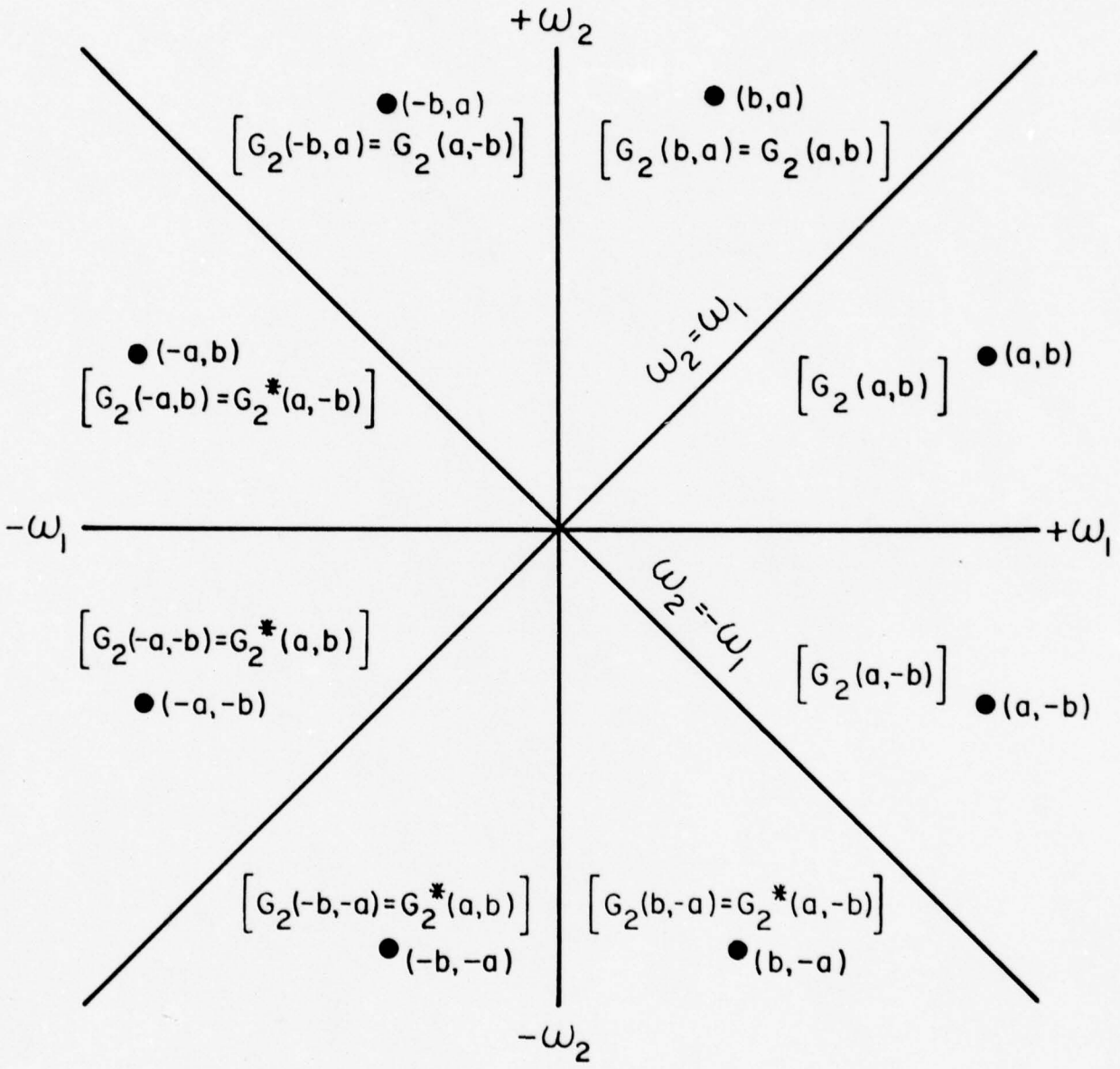

FIGURE 1a. SYMMETRY OF THE QUADRATIC FREQUENCY RESPONSE FUNCTION

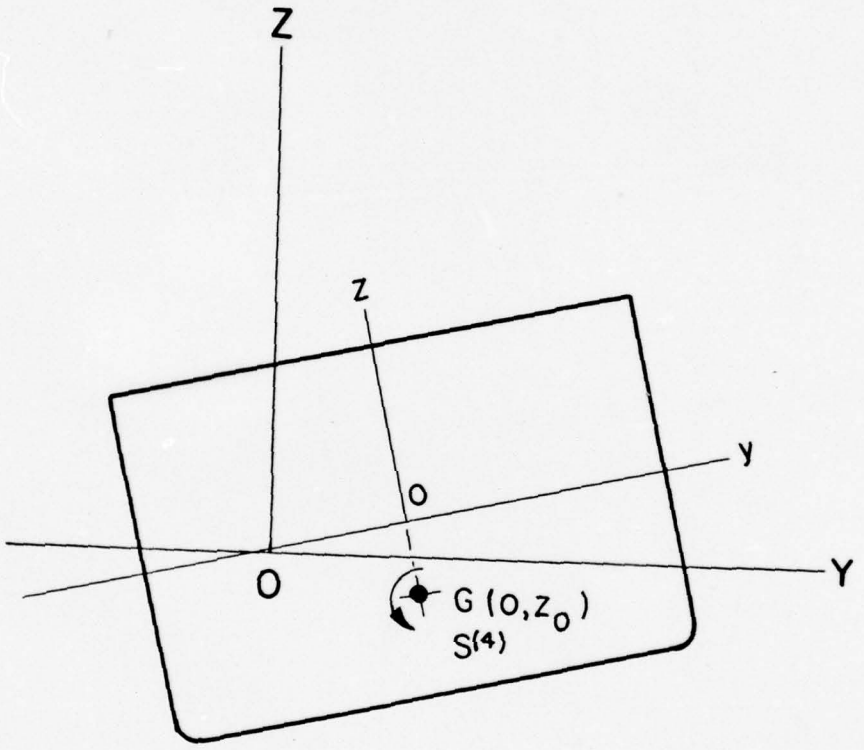

FIG. I-b. SKETCH OF THE COORDINATE SYSTEMS

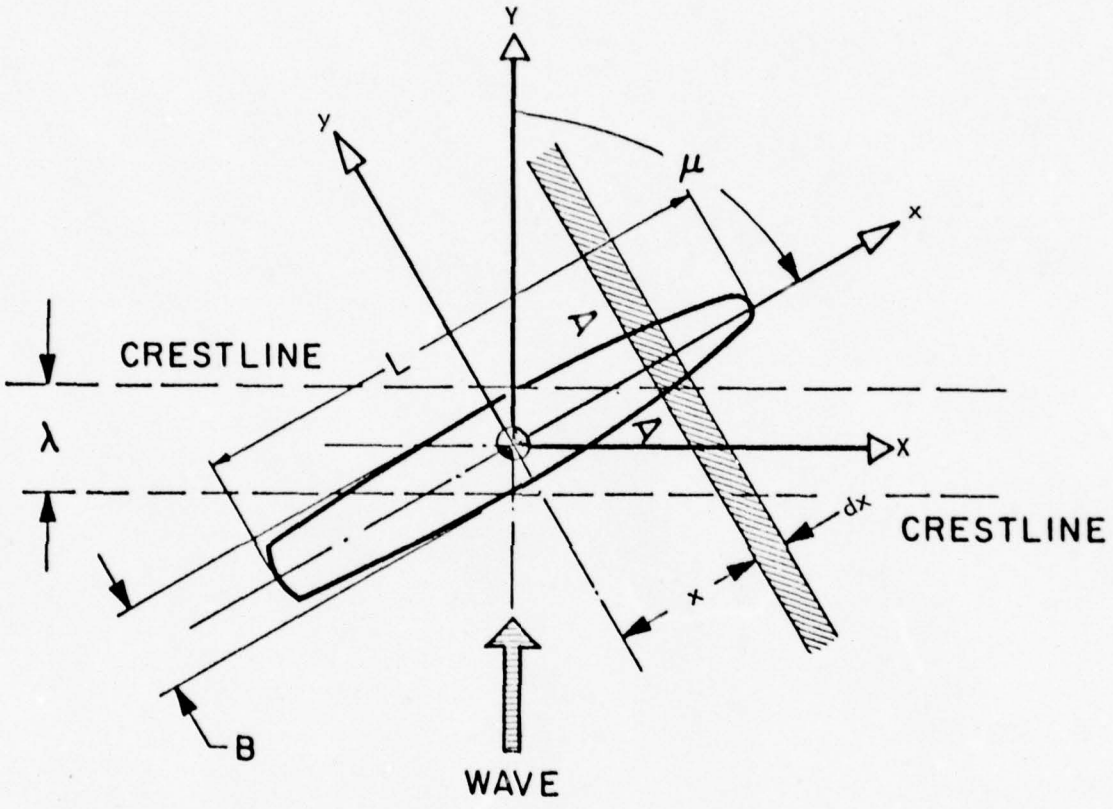

FIGURE 1c. SKETCH OF COORDINATE SYSTEMS

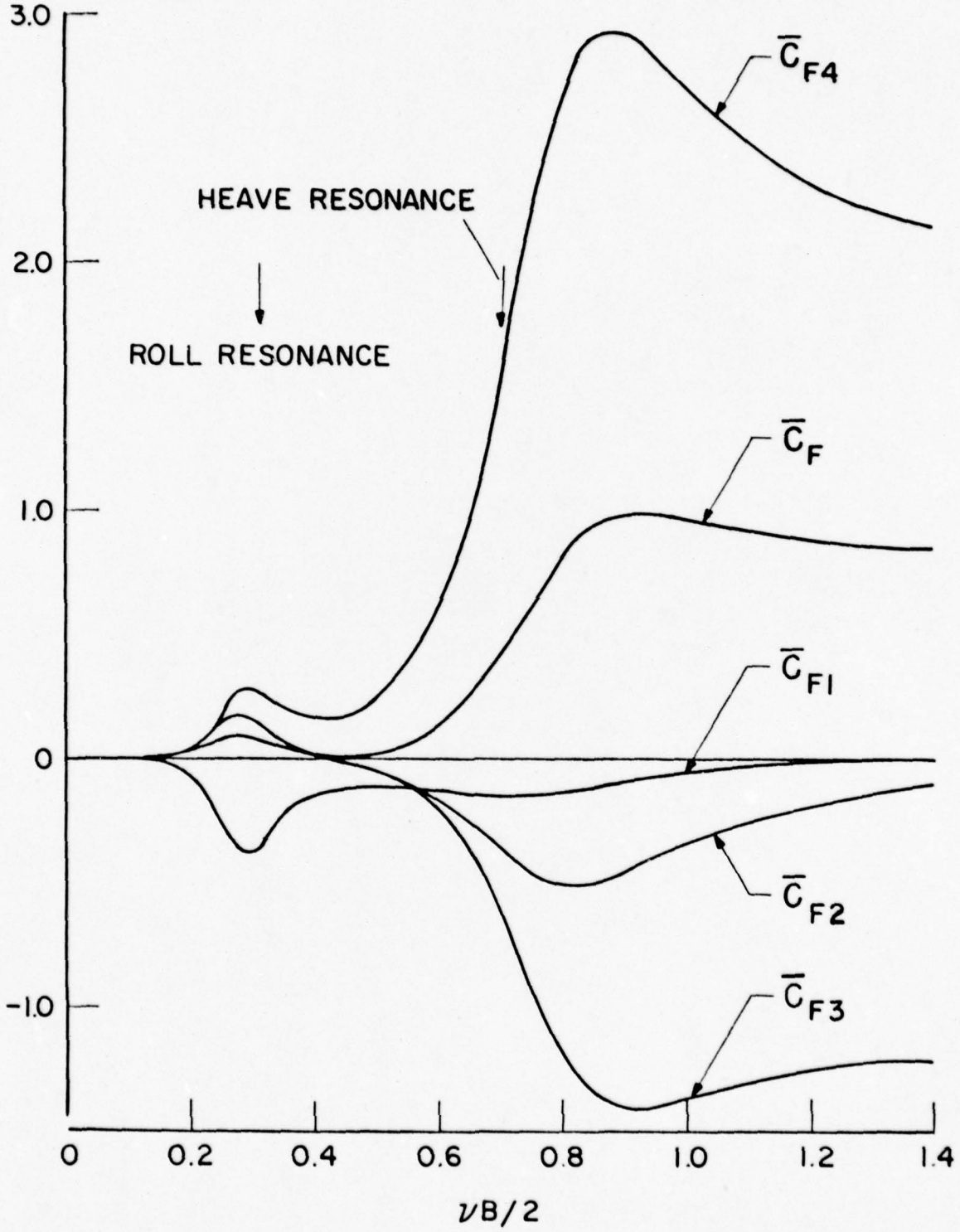

FIG. 2a. THE FOUR COMPONENTS OF THE MEAN DRIFTING FORCE ON THE CYLINDER

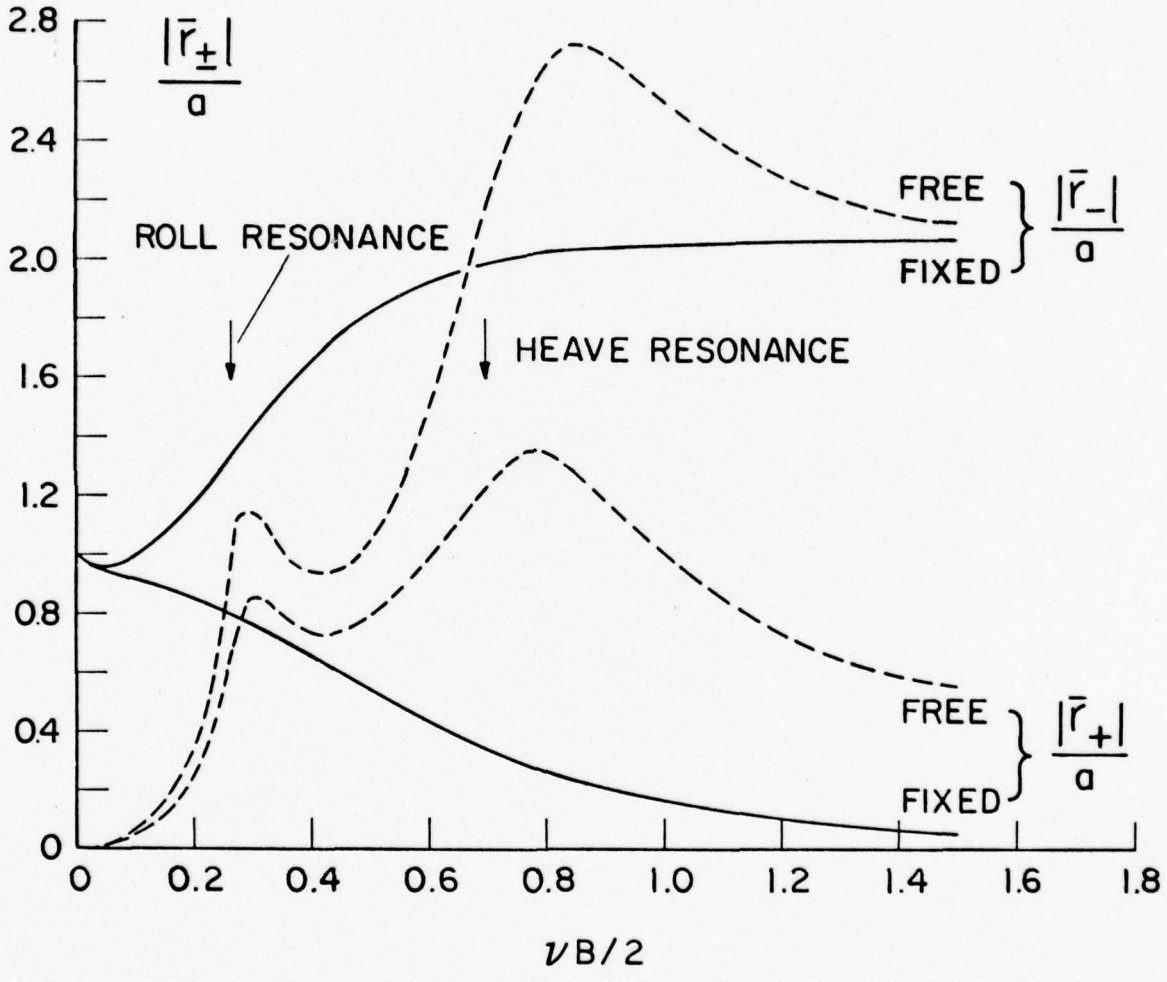

FIG. 2b. THE RELATIVE WAVE ELEVATION

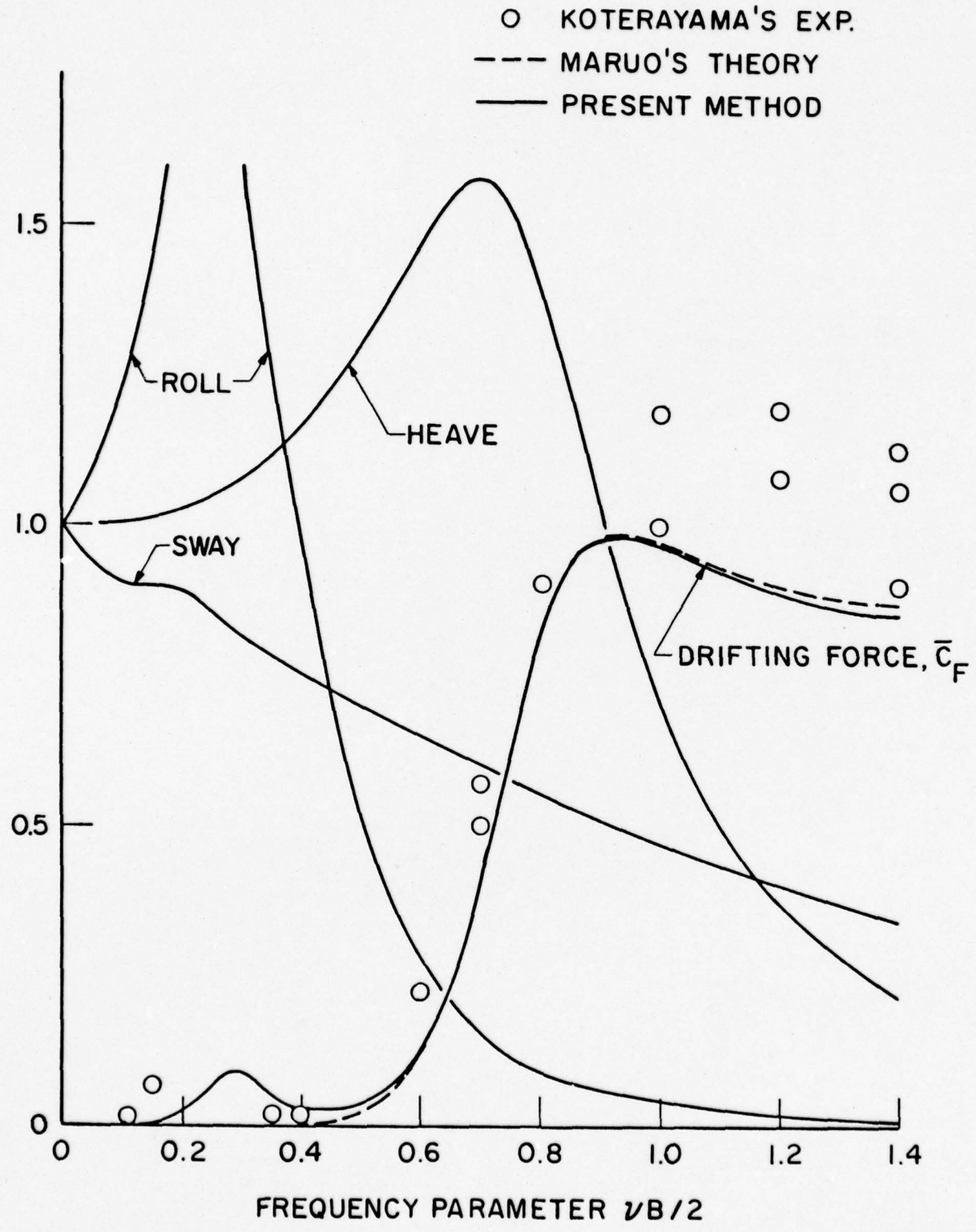

FIG. 2c. THE MEAN DRIFTING FORCE OF A FREE CYLINDER

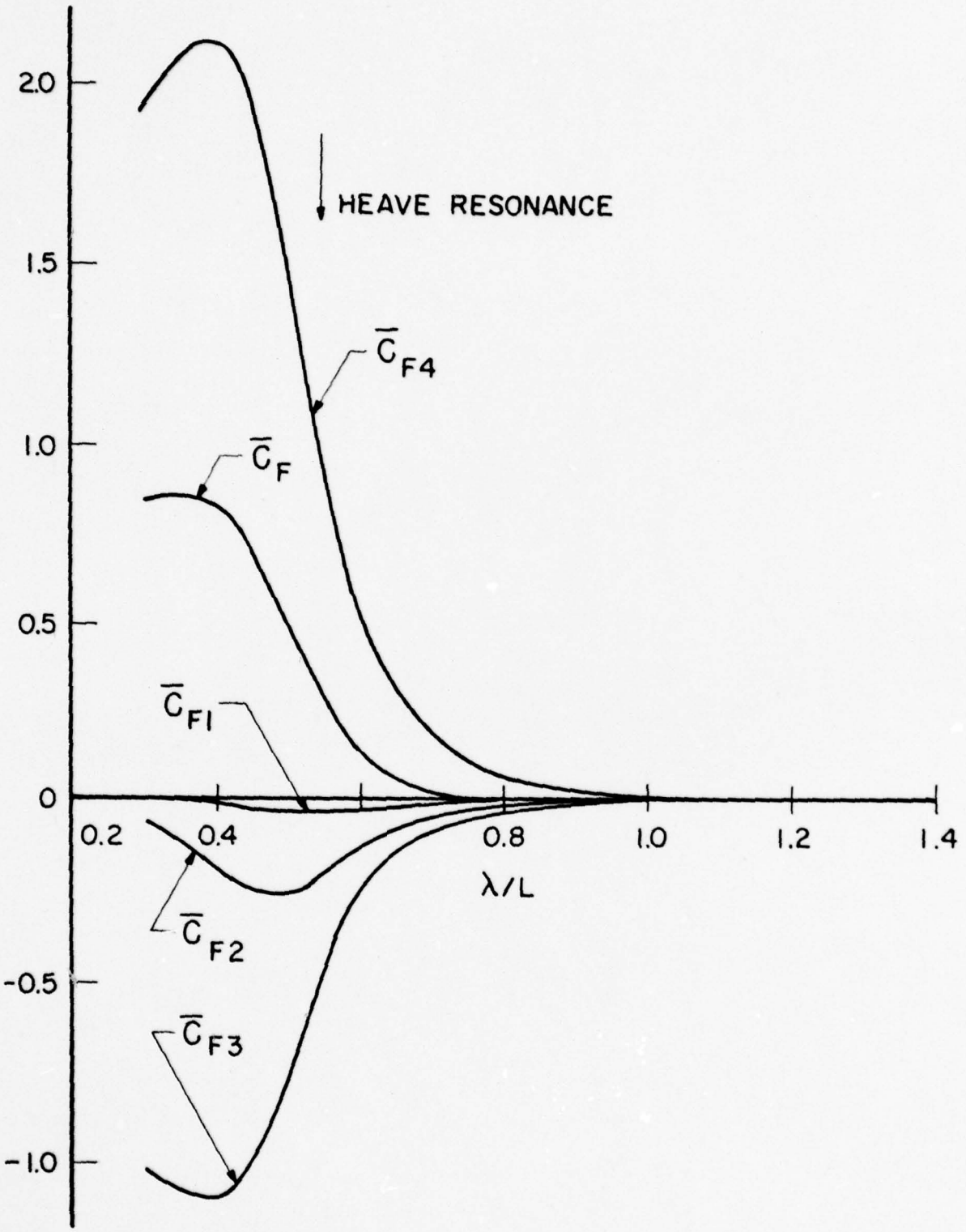

FIG. 3a. THE FOUR COMPONENTS OF THE MEAN DRIFTING FORCE ON THE SHIP MODEL IN BEAM SEAS ($\mu = 90°$)

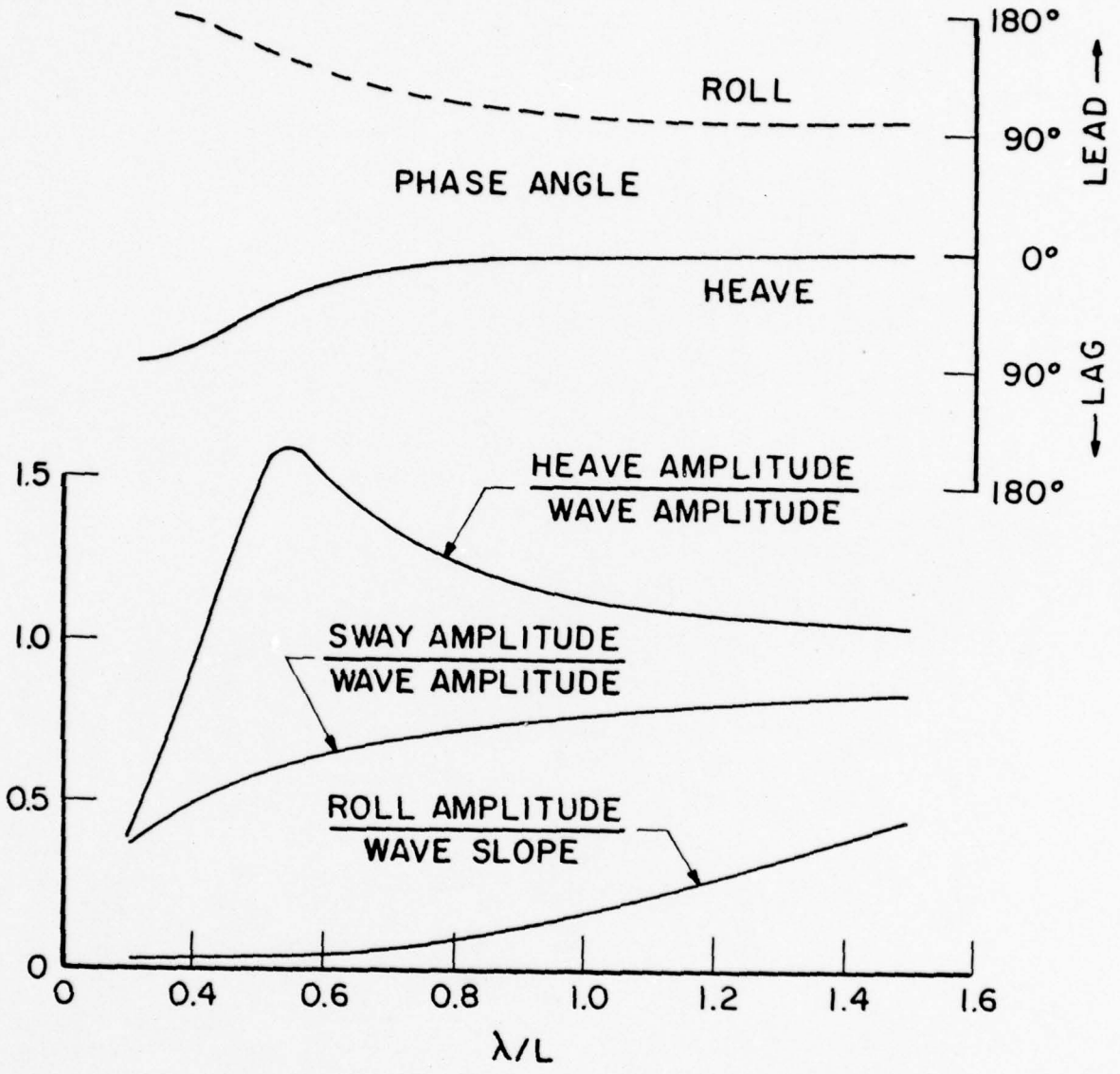

FIG. 3b. SWAY, HEAVE AND ROLL RESPONSES OF THE SHIP MODEL IN BEAM SEAS ($\mu = 90°$)

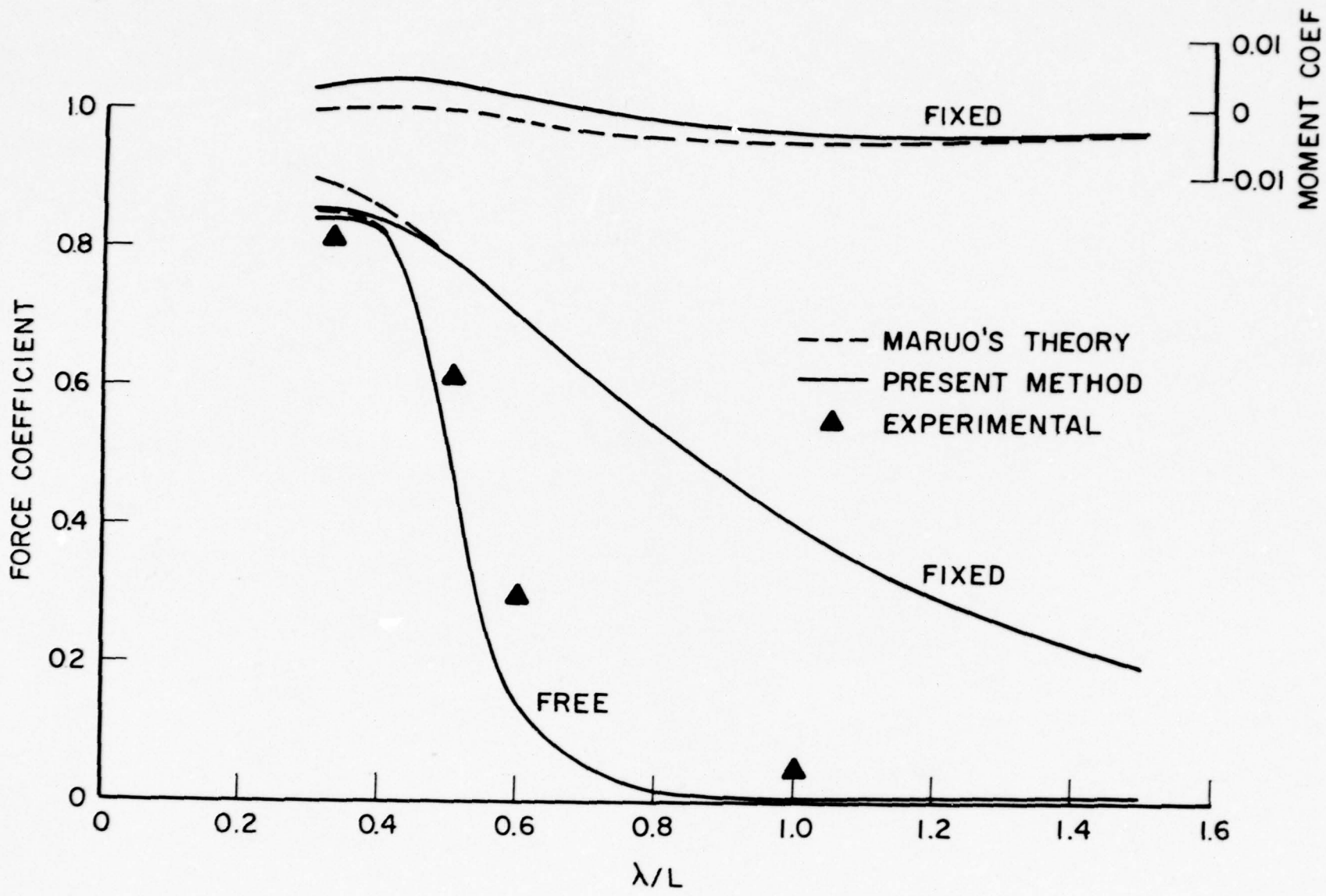

R-2061

FIG. 3c. THE MEAN DRIFTING FORCE AND MOMENT ON THE SHIP MODEL IN BEAM SEAS ($\mu = 90°$)

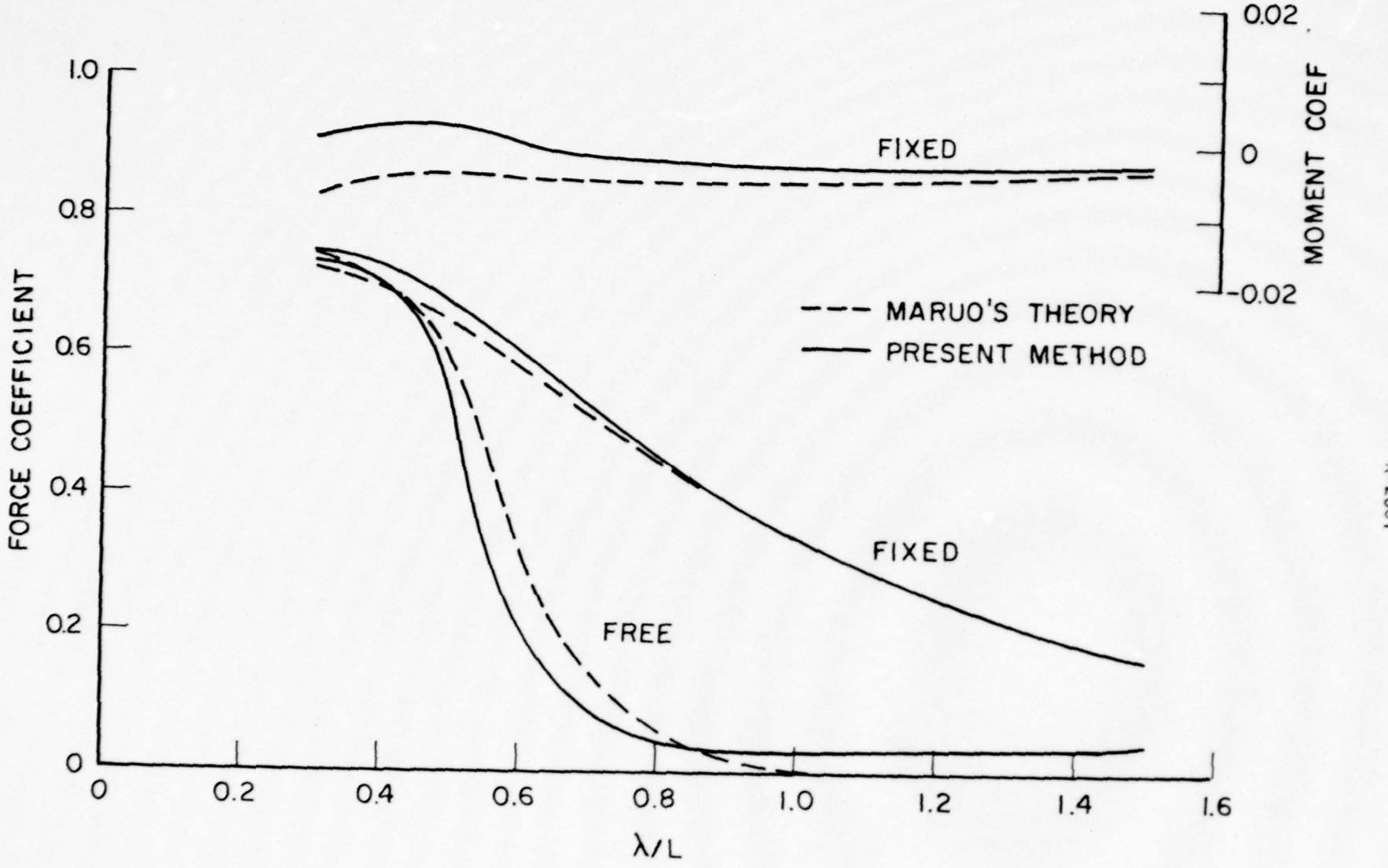

FIG. 3d. THE MEAN DRIFTING FORCE ON THE SHIP MODEL IN QUARTERING SEAS (μ=60°)

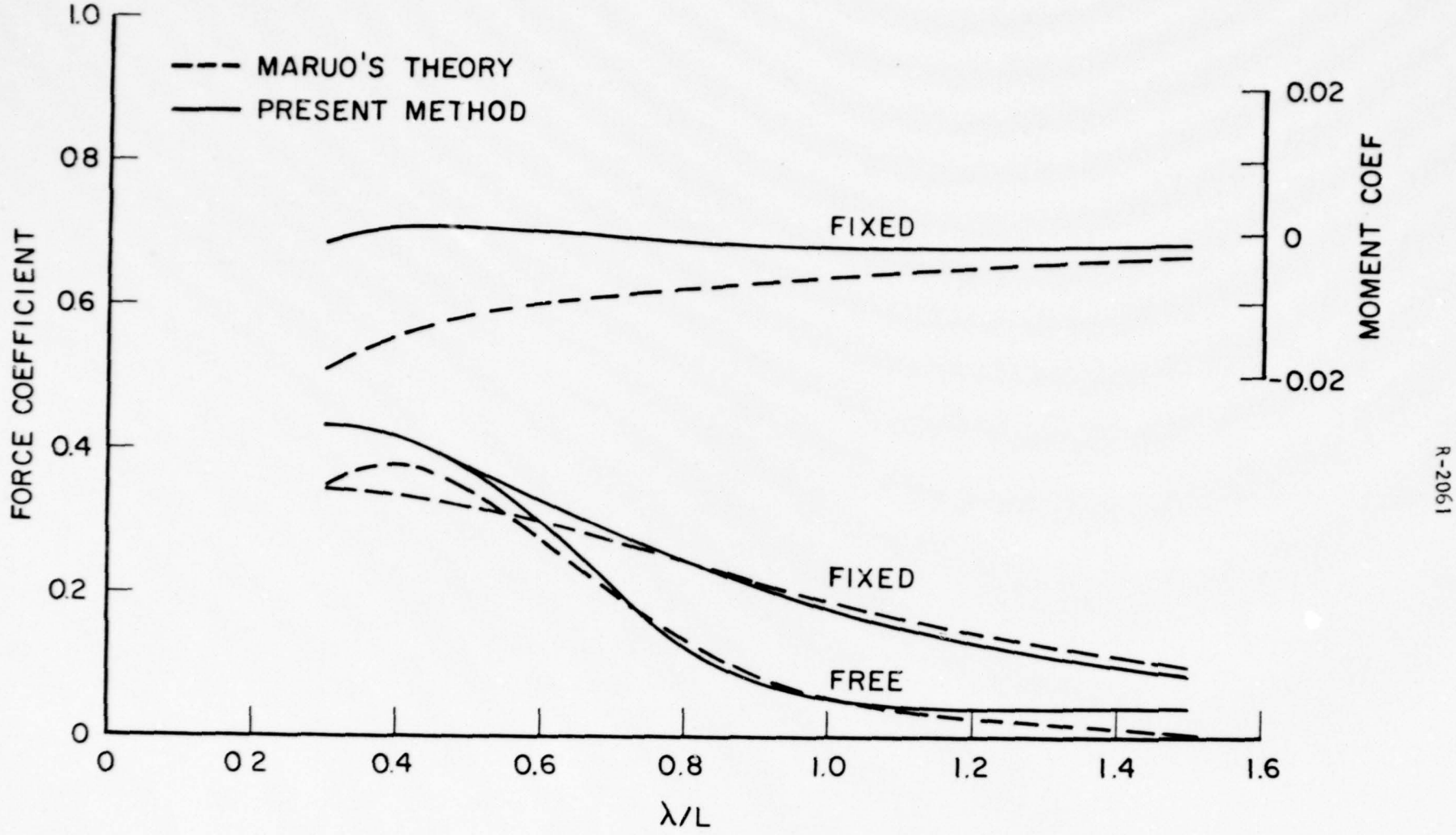

FIG. 3e. THE MEAN DRIFTING FORCE AND MOMENT ON THE SHIP MODEL IN QUARTERING SEAS (μ=30°)

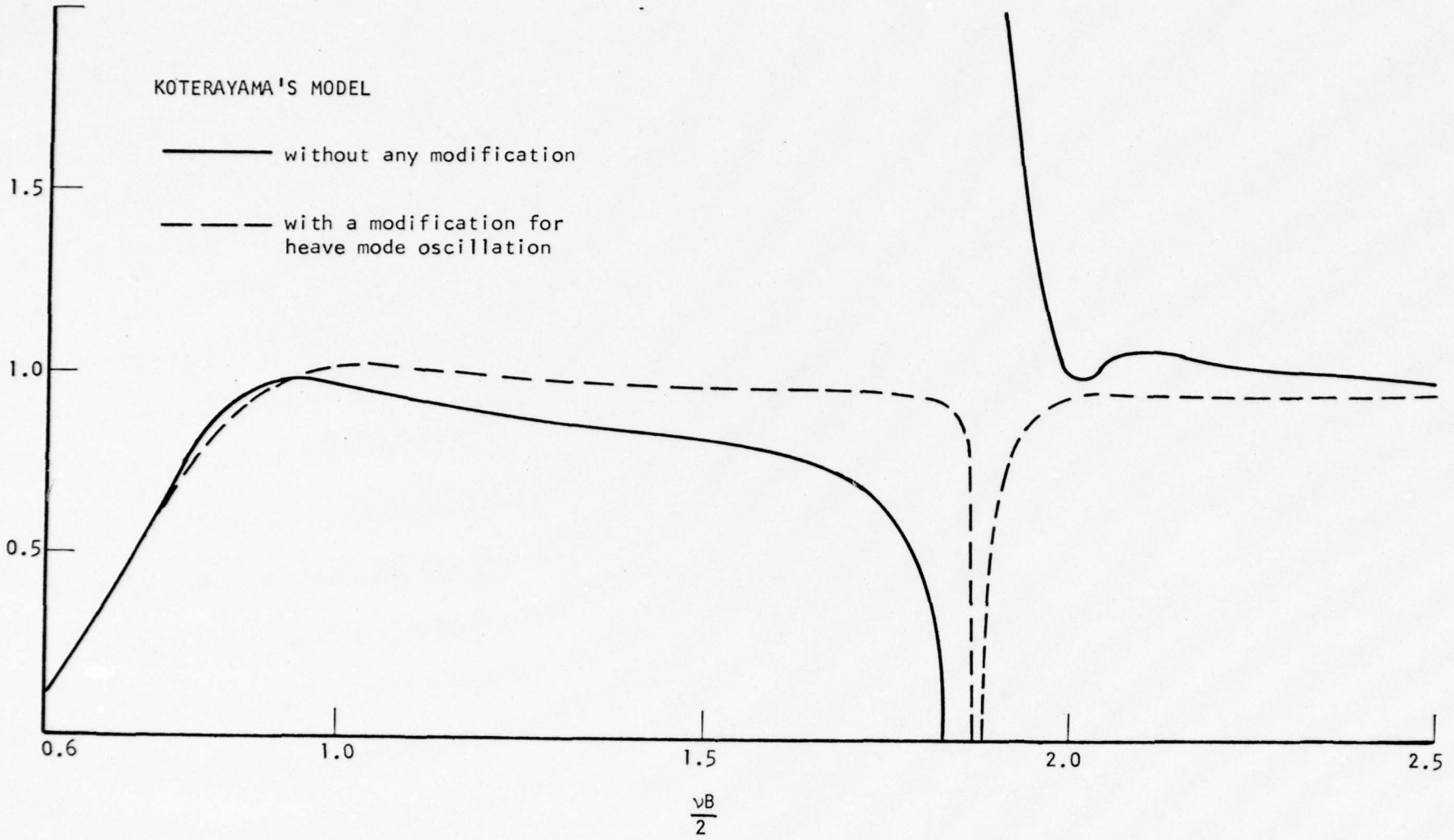

FIGURE 4. THE IRREGULAR FREQUENCY PHENOMENON IN THE MEAN LATERAL DRIFTING FORCE COEFFICIENT OF A CYLINDER

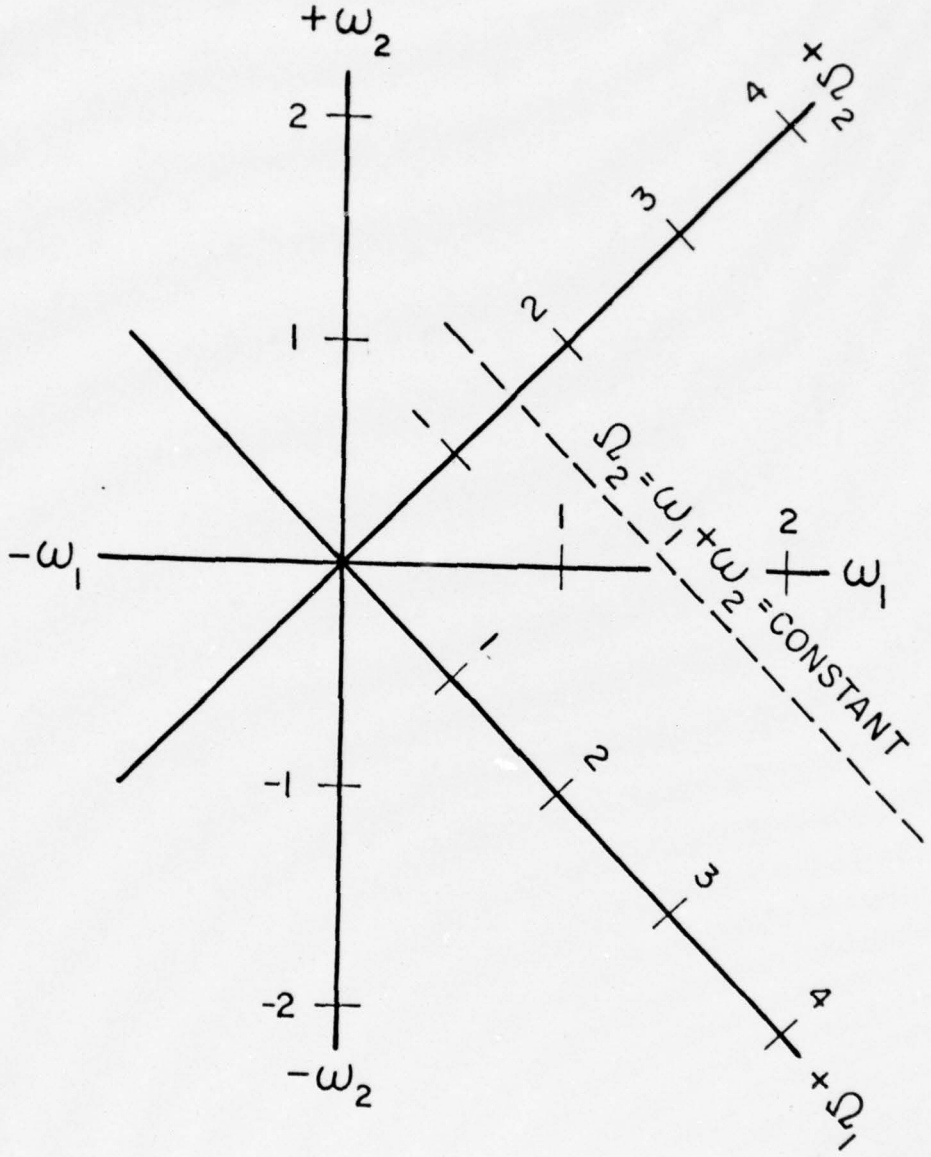

FIGURE 5 MAPPING OF THE Ω_1, Ω_2 PLANE

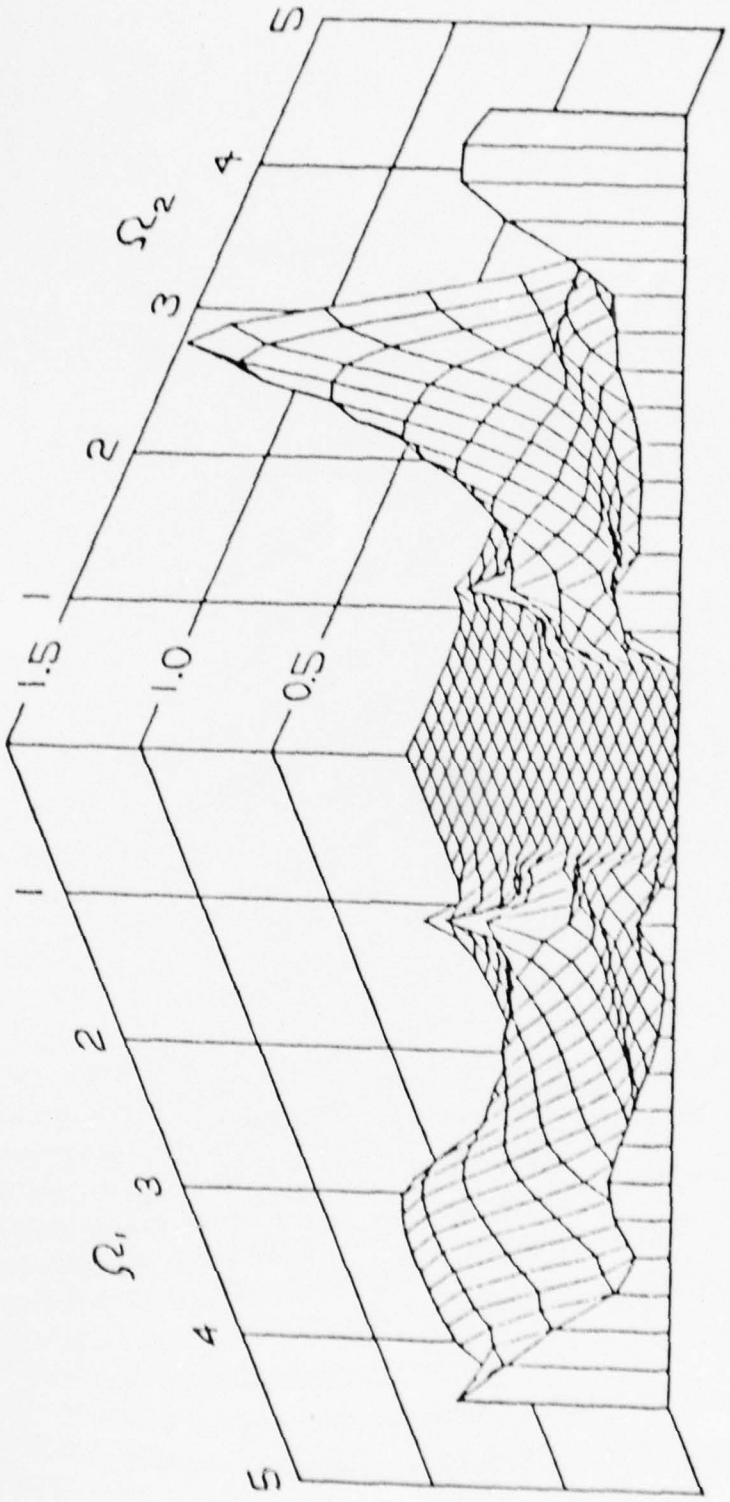

FIGURE 6. ISOMETRIC VIEW OF THE MODULUS OF THE ANALYTICALLY ESTIMATED QUADRATIC FREQUENCY RESPONSE FUNCTION FOR THE LATERAL DRIFTING FORCE OF A SHIP AT 60° HEADING

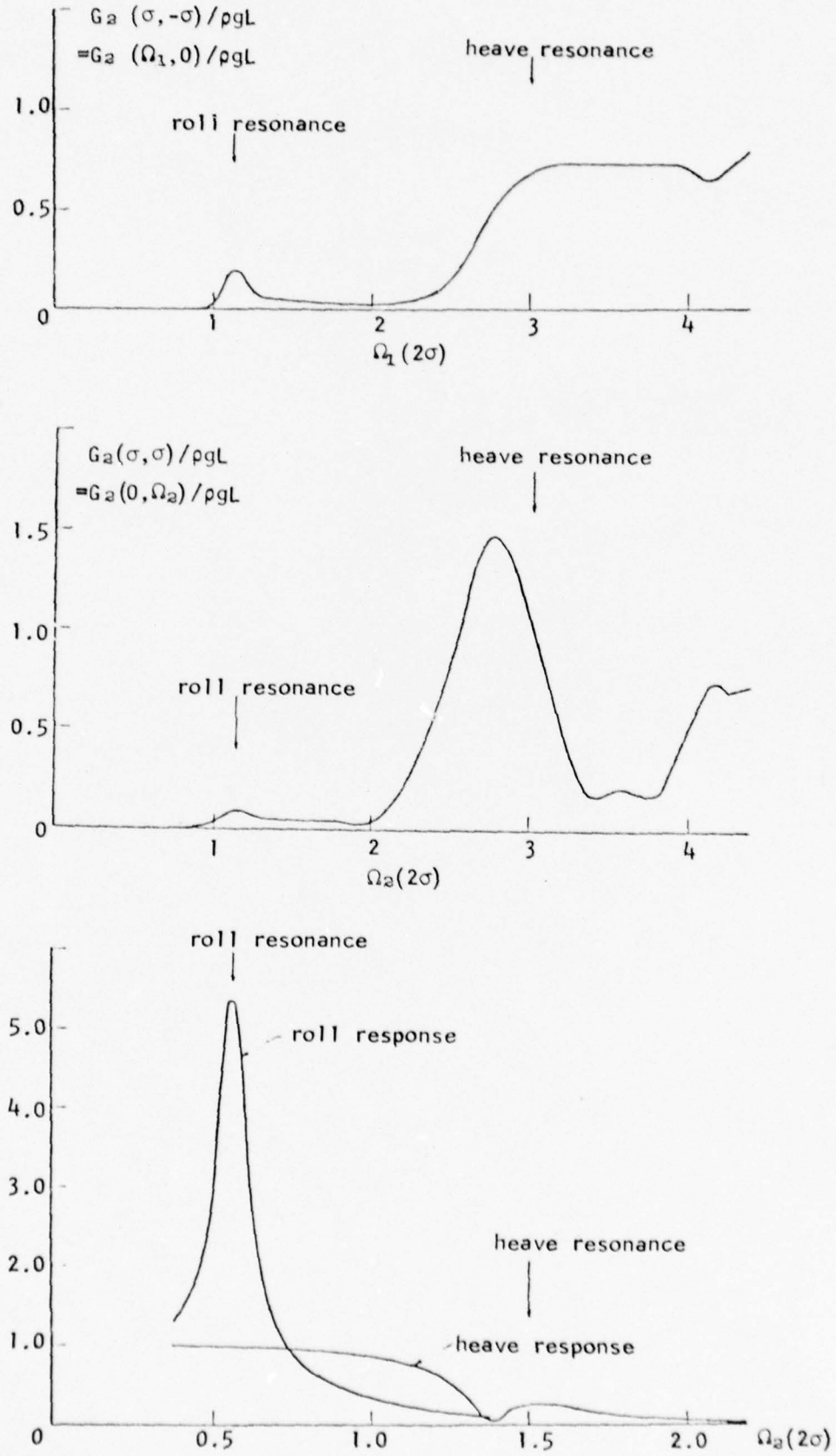

FIGURE 7. MODULI OF THE QUADRATIC FREQUENCY RESPONSES FOR THE LATERAL DRIFTING FORCES OF A SHIP AT 60° HEADING

APPENDIX A

THE $H_{l,k}$ FUNCTIONS FOR THE LATERAL DRIFTING FORCE

1) $\underline{H_{1,1} \text{ for } I_1}$

$$I_1 = \mathrm{Re}\left\{\sum_{m=1,2} \frac{\bar{S}^{(4)}(\omega_m)}{a_m} e^{-i\omega_m t}\right\} \mathrm{Re}\left\{\int_L dx\, m_o(x) \sum_{n=1,2} \omega_n^2 \frac{\bar{S}^{(3)}(x,\omega_n)}{a_n} e^{-i\omega_n t}\right\} \tag{A-1}$$

$$H_{1,1}(\omega_m,\omega_n) = \frac{\bar{S}^{(4)}(\omega_m)}{a_m} \int_L dx\, m_o(x)\, \omega_n^2 \frac{\bar{S}^{(3)}(x,\omega_n)}{a_n} \tag{A-2}$$

Since $\bar{S}^{(3)}(x,\omega) = S^{(3)}(\omega) - x\, S^{(5)}(\omega)$,

$$\int_L m_o(x)dx = M_o \quad \text{(ship mass)} \; ; \; \int_L x\, m_o(x)dx = 0 \tag{A-3}$$

we have

$$\int_L dx\, m_o(x)\omega_n^2 \frac{\bar{S}^{(3)}(x,\omega_n)}{a_m} = \omega_n^2 M_o \frac{\bar{S}^{(3)}(\omega_n)}{a_n}$$

thus,

$$\mathrm{Re}\, H_{1,1}(\omega_m,\pm\omega_n) = \frac{S_c^{(4)}(\omega_m)}{a_m} \omega_n^2 \frac{S_c^{(3)}(\omega_n)}{a_n} M_o \mp \frac{S_s^{(4)}(\omega_m)}{a_m} \omega_n^2 \frac{S_s^{(3)}(\omega_n)}{a_n} M_o \tag{A-4}$$

$$\mathrm{Im}\, H_{1,1}(\omega_m,\pm\omega_n) = \pm \frac{S_c^{(4)}(\omega_m)}{a_m} \omega_n^2 \frac{S_s^{(3)}(\omega_n)}{a_n} M_o + \frac{S_s^{(4)}(\omega_m)}{a_m} \omega_n^2 \frac{S_c^{(3)}(\omega_n)}{a_n} M_o \tag{A-5}$$

2) $H_{1,2}$ for I_2

$$I_2 = \mathrm{Re}\left\{\int_L dx \sum_{m=1,2} \frac{\bar{S}^{(4)}(x,\omega_m)}{a_m} e^{-i\omega_m t}\right\} \mathrm{Re}\left\{\int_{c(x)} dz \sum_{n=1,2} \rho \frac{\partial}{\partial t}\left(\frac{\bar{\varphi}_y(\omega_n)}{a_n} e^{-i\omega_n t}\right) dz\right\} \tag{A-6}$$

$$H_{1,2}(\omega_m,\omega_n) = \int_L dx \frac{\bar{S}^{(2)}(x,\omega_m)}{a_m} \int_{c(x)} \rho\omega_n \left(\frac{\varphi_{ys}(\omega_n)}{a_n} - i \frac{\varphi_{yc}(\omega_n)}{a_n}\right) dz \tag{A-7}$$

$$\begin{aligned}
\mathrm{Re}\, H_{1,2} = {} & \frac{S_c^{(2)}(\omega_m)}{a_m} \int_L dx\, \rho\, \omega_n \int_{c(x)} \frac{\varphi_{ys}(\omega_n)}{a_n} dz \\
& + \frac{S_c^{(6)}(\omega_m)}{a_m} \int_L dx\, x\, \rho\, \omega_n \int_{c(x)} \frac{\varphi_{ys}(\omega_n)}{a_n} dz \\
& \pm \frac{S_s^{(2)}(\omega_m)}{a_m} \int_L dx\, \rho\, \omega_n \int_{c(x)} \frac{\varphi_{yc}(\omega_n)}{a_n} dz \\
& \pm \frac{S_s^{(6)}(\omega_m)}{a_m} \int_L dx\, x\, \rho\, \omega_n \int_{c(x)} \frac{\varphi_{yc}(\omega_n)}{a_n} dz
\end{aligned} \tag{A-8}$$

$$\begin{aligned}
\mathrm{Im}\, H_{1,2} = {} & \mp \frac{S_c^{(2)}(\omega_m)}{a_m} \int_L dx\, \rho\, \omega_n \int_{c(x)} \frac{\varphi_{yc}(\omega_n)}{a_n} dz \\
& \mp \frac{S_c^{(6)}(\omega_m)}{a_m} \int_L dx\, x\, \rho\, \omega_n \int_{c(x)} \frac{\varphi_{yc}(\omega_n)}{a_n} dz \\
& + \frac{S_s^{(2)}(\omega_m)}{a_m} \int_L dx\, \rho\, \omega_n \int_{c(x)} \frac{\varphi_{ys}(\omega_n)}{a_n} dz \\
& + \frac{S_s^{(6)}(\omega_m)}{a_m} \int_L dx\, x\, \rho\, \omega_n \int_{c(x)} \frac{\varphi_{ys}(\omega_n)}{a_n} dz
\end{aligned} \tag{A-9}$$

3) $H_{1,3}$ for I_3

$$I_3 = \mathrm{Re}\left\{ - \sum_{m=1,2} \frac{\bar{S}^{(4)}(\omega_m)}{a_m} e^{-i\omega_m t} \right\} \mathrm{Re}\left\{ \int_L dx \int_{c(x)} (z-z_o) \sum_{n=1,2} \rho \frac{\partial}{\partial t} \left(\frac{\bar{\varphi}_y(\omega_n)}{a_n} e^{-i\omega_n t} \right) dz \right\} \tag{A-10}$$

$$H_{1,3}(\omega_m, \omega_n) = - \frac{\bar{S}^{(4)}(\omega_m)}{a_m} \int_L dx\ \rho\omega_n \int_{c(x)} (z-z_o) \left(\frac{\varphi_{ys}(\omega_n)}{a_n} - i \frac{\varphi_{yc}(\omega_n)}{a_n} \right) dz \tag{A-11}$$

$$\mathrm{Re}\ H_{1,3} = - \frac{S_c^{(4)}(\omega_m)}{a_m} \int_L dx\ \rho\omega_n \int_{c(x)} (z-z_o) \frac{\varphi_{ys}(\omega_n)}{a_n} dz$$

$$\mp \frac{S_s^{(4)}(\omega_m)}{a_m} \int_L dx\ \rho\omega_n \int_{c(x)} (z-z_o) \frac{\varphi_{yc}(\omega_n)}{a_n} dz \tag{A-12}$$

$$\mathrm{Im}\ H_{1,3} = \pm \frac{S_c^{(4)}(\omega_m)}{a_m} \int_L dx\ \rho\omega_n \int_{c(x)} (z-z_o) \frac{\varphi_{yc}(\omega_n)}{a_n} dz$$

$$- \frac{S_s^{(4)}(\omega_m)}{a_m} \int_L dx\ \rho\omega_n \int_{c(x)} (z-z_o) \frac{\varphi_{ys}(\omega_n)}{a_n} dz \tag{A-13}$$

4) $H_{1,4}$ for I_4

$$I_4 = \mathrm{Re}\left\{ \int_L dx \sum_{m=1,2} \frac{\bar{S}^{(3)}(x,\omega_m)}{a_m} e^{-i\omega_m t} \right\} \mathrm{Re}\left\{ \int_{c(x)} \rho \sum_{n=1,2} \frac{\partial}{\partial t} \left(\frac{\bar{\varphi}_z(\omega_n)}{a_n} e^{-i\omega_n t} \right) dz \right\} \tag{A-14}$$

$$H_{1,4}(\omega_m, \omega_n) = \int_L dx \left(\frac{\bar{S}^{(3)}(\omega_m)}{a_n} - x \frac{\bar{S}^{(5)}(\omega_m)}{a_n} \right) \int_{c(x)} \rho\omega_n \left(\frac{\varphi_{zs}(\omega_n)}{a_n} - i \frac{\varphi_{zc}(\omega_n)}{a_n} \right) dz \tag{A-15}$$

$$\text{Re } H_{1,4} = \frac{S_c^{(3)}(\omega_m)}{a_m} \int_L dx\ \rho\omega_n \int_{c(x)} \frac{\varphi_{zs}(\omega_n)}{a_n} dz$$

$$- \frac{S_c^{(5)}(\omega_m)}{a_m} \int_L dx \times \rho\omega_n \int_{c(x)} \frac{\varphi_{zs}(\omega_n)}{a_n} dz$$

$$\pm \frac{S_s^{(3)}(\omega_m)}{a_m} \int_L dx\ \rho\omega_n \int_{c(x)} \frac{\varphi_{zc}(\omega_n)}{a_n} dz$$

$$\mp \frac{S_s^{(5)}(\omega_m)}{a_m} \int_L dx \times \rho\omega_n \int_{c(x)} \frac{\varphi_{zc}(\omega_n)}{a_n} dz \qquad \text{(A-16)}$$

$$\text{Im } H_{1,4} = \mp \frac{S_c^{(3)}(\omega_m)}{a_m} \int_L dx\ \rho\omega_n \int_{c(x)} \frac{\varphi_{zc}(\omega_n)}{a_n} dz$$

$$\pm \frac{S_c^{(5)}(\omega_m)}{a_m} \int_L dx \times \rho\omega_n \int_{c(x)} \frac{\varphi_{zc}(\omega_n)}{a_n} dz$$

$$+ \frac{S_s^{(3)}(\omega_m)}{a_m} \int_L dx\ \rho\omega_n \int_{c(x)} \frac{\varphi_{zs}(\omega_n)}{a_n} dz$$

$$- \frac{S_s^{(5)}(\omega_m)}{a_m} \int_L dx \times \rho\omega_n \int_{c(x)} \frac{\varphi_{zs}(\omega_n)}{a_n} dz \qquad \text{(A-17)}$$

5) $H_{1,5}$ for I_5

$$I_5 = \text{Re}\left\{ \sum_{m=1,2} \frac{\bar{S}^{(4)}(\omega_m)}{a_m} e^{-i\omega_m t} \right\} \text{Re}\left\{ \int_L dx \int_{c(x)} y\rho \sum_{n=1,2} \frac{\partial}{\partial t}\left(\frac{\bar{\varphi}_z(\omega_n)}{a_n} e^{-i\omega_n t} \right) dz \right\} \qquad \text{(A-18)}$$

$$H_{1,5}(\omega_m, \omega_n) = \frac{\bar{S}^{(4)}(\omega_m)}{a_m} \int_L dx\ \rho\omega_n \int_{c(x)} y \left(\frac{\varphi_{zs}(\omega_n)}{a_n} - i \frac{\varphi_{zc}(\omega_n)}{a_n} \right) dz \qquad \text{(A-19)}$$

$$\text{Re } H_{1,5} = \frac{S_c^{(4)}(\omega_m)}{a_m} \int_L dx\ \rho\omega_n \int_{c(x)} y\ \frac{\varphi_{zs}(\omega_n)}{a_n}\, dz$$

$$\pm \frac{S_s^{(4)}(\omega_m)}{a_m} \int_L dx\ \rho\omega_n \int_{c(x)} y\ \frac{\varphi_{zc}(\omega_n)}{a_n}\, dz \qquad \text{(A-20)}$$

$$\text{Im } H_{1,5} = \mp \frac{S_c^{(4)}(\omega_m)}{a_m} \int_L dx\ \rho\omega_n \int_{c(x)} y\ \frac{\varphi_{zc}(\omega_n)}{a_n}\, dz$$

$$+ \frac{S_s^{(4)}(\omega_m)}{a_m} \int_L dx\ \rho\omega_m \int_{c(x)} y\ \frac{\varphi_{zs}(\omega_n)}{a_n}\, dz \qquad \text{(A-21)}$$

6) $\underline{H_{1,6} \text{ for } I_6}$

$$I_6 = \frac{1}{2}\rho \int_L dx \int_{c(x)} \text{Re}\left\{ \sum_{m=1,2} \frac{\nabla\bar{\varphi}(\omega_m)}{a_m} e^{-i\omega_m t} \right\} \text{Re}\left\{ \sum_{n=1,2} \frac{\nabla\bar{\varphi}(\omega_n)}{a_n} e^{-i\omega_n t} \right\} dz \qquad \text{(A-22)}$$

$$H_{1,6}(\omega_m,\omega_n) = \frac{1}{2}\rho \int_L dx \int_{c(x)} \frac{\nabla\bar{\varphi}(\nabla_m)}{a_m} \quad \frac{\nabla\bar{\varphi}(\omega_n)}{a_n}\, dz \quad . \qquad \text{(A-23)}$$

$$\text{Re } H_{1,6} = \frac{\rho}{2} \int_L dx \int_{c(x)} \left[\frac{\varphi_{yc}(\omega_m)}{a_m} \frac{\varphi_{yc}(\omega_n)}{a_n} + \frac{\varphi_{zc}(\omega_m)}{a_m} \frac{\varphi_{zc}(\omega_n)}{a_n} \right] dz$$

$$\mp \frac{\rho}{2} \int_L dx \int_{c(x)} \left[\frac{\varphi_{ys}(\omega_m)}{a_m} \frac{\varphi_{ys}(\omega_n)}{a_n} + \frac{\varphi_{zs}(\omega_m)}{a_m} \frac{\varphi_{zs}(\omega_n)}{a_n} \right] dz \qquad \text{(A-24)}$$

$$\text{Im } H_{1,6} = \pm \frac{\rho}{2} \int_L dx \int_{c(x)} \left[\frac{\varphi_{yc}(\omega_m)}{a_m} \frac{\varphi_{ys}(\omega_n)}{a_n} + \frac{\varphi_{zc}(\omega_m)}{a_m} \frac{\varphi_{zs}(\omega_n)}{a_n} \right] dz$$

$$+ \frac{\rho}{2} \int_L dx \int_{c(x)} \left[\frac{\varphi_{ys}(\omega_m)}{a_m} \frac{\varphi_{yc}(\omega_n)}{a_n} + \frac{\varphi_{zs}(\omega_m)}{a_m} \frac{\varphi_{zc}(\omega_n)}{a_n} \right] dz \qquad \text{(A-25)}$$

The velocity components of the water are evaluated by applying formula (C-19) in Appendix C.

7) $H_{1,7}$ for I_7

$$I_7 = \frac{1}{2}\rho g \int_L dx\Big\{-\mathrm{Re}\Big(\sum_{m=1,2}\frac{\bar{r}_+(\omega_m)}{a_m}e^{-i\omega_m t}\Big)\mathrm{Re}\Big(\sum_{n=1,2}\frac{\bar{r}_+(\omega_n)}{a_n}e^{-i\omega_n t}\Big)$$

$$+\mathrm{Re}\Big(\sum_{m=1,2}\frac{\bar{r}_-(\omega_m)}{a_m}e^{-i\omega_m t}\Big)\mathrm{Re}\Big(\sum_{n=1,2}\frac{\bar{r}_-(\omega_n)}{a_n}e^{-i\omega_n t}\Big)\Big\} \qquad \text{(A-26)}$$

$$H_{1,7}(\omega_m,\omega_n) = \frac{1}{2}\rho g \int_L dx\left\{-\frac{\bar{r}_+(\omega_m)}{a_m}\frac{\bar{r}_+(\omega_n)}{a_n} + \frac{\bar{r}_-(\omega_m)}{a_m}\frac{\bar{r}_-(\omega_n)}{a_n}\right\} \qquad \text{(A-27)}$$

$$\mathrm{Re}\ H_{1,7} = \frac{1}{2}\rho g \int_L dx\left\{-\frac{r_{c+}(\omega_m)}{a_m}\frac{r_{c+}(\omega_n)}{a_n} \pm \frac{r_{s+}(\omega_m)}{a_m}\frac{r_{s+}(\omega_n)}{a_n}\right.$$

$$\left. + \frac{r_{c-}(\omega_m)}{a_m}\frac{r_{c-}(\omega_n)}{a_n} \mp \frac{r_{s-}(\omega_m)}{a_m}\frac{r_{s-}(\omega_n)}{a_n}\right\} \qquad \text{(A-28)}$$

$$\mathrm{Im}\ H_{1,7} = \frac{1}{2}\rho g \int_L dx\left\{\mp\frac{r_{c+}(\omega_m)}{a_m}\frac{r_{s+}(\omega_n)}{a_n} - \frac{r_{s+}(\omega_m)}{a_m}\frac{r_{c+}(\omega_n)}{a_n}\right.$$

$$\left. \pm \frac{r_{c-}(\omega_m)}{a_m}\frac{r_{s-}(\omega_n)}{a_n} + \frac{r_{s-}(\omega_m)}{a_m}\frac{r_{c-}(\omega_n)}{a_n}\right\} \qquad \text{(A-29)}$$

where

$$\frac{r_{c\pm}(x,\omega_m)}{a_m} = -\frac{\rho\omega_m\varphi_{s\pm}(\omega_m)}{\rho g a_m} - \frac{S_c^{(3)}(\omega_m)}{a_m} + x\frac{S_c^{(5)}(\omega_m)}{a_m} \mp \frac{B(x)}{2}\frac{S_c^{(4)}(\omega_m)}{a_m}$$

$$\frac{r_{s\pm}(x,\omega_m)}{a_m} = \frac{\rho\omega_m\varphi_{c\pm}(\omega_m)}{\rho g a_m} - \frac{S_s^{(3)}(\omega_m)}{a_m} + x\frac{S_s^{(5)}(\omega_m)}{a_m} \mp \frac{B(x)}{2}\frac{S_s^{(4)}(\omega_m)}{a_m} \qquad \text{(A-30)}$$

$$\left.\begin{aligned} -\frac{\rho\omega_m\varphi_{s\pm}(\omega_m)}{\rho g a_m} &= \frac{p_c}{\rho g a_m} \\ \frac{\rho\omega_m\varphi_c(\omega_m)}{\rho g a_m} &= \frac{p_s}{\rho g a_m} \end{aligned}\right\} \quad y = \pm B/2\ ,\ z = 0\ . \qquad \text{(A-31)}$$

Formulas (A-30) and (A-31) are evaluated by employing (C-17) in Appendix C.

APPENDIX B

THE $H_{1,k}$ FUNCTIONS FOR THE LATERAL DRIFTING MOMENT

1) $\underline{H_{1,1} \text{ for } I_1}$

$$I_1 = \mathrm{Re}\left\{ \sum_{m=1,2} \frac{\bar{S}^{(4)}(\omega_m)}{a_m} e^{-i\omega_m t} \right\} \mathrm{Re}\left\{ \int_L dx \times m_o(x) \sum_{n=1,2} \omega_n^2 \frac{\bar{S}^{(3)}(x,\omega_n)}{a_n} e^{-i\omega_n t} \right\} \tag{B-1}$$

$$H_{1,1}(\omega_m,\omega_n) = \frac{\bar{S}^{(4)}(\omega_m)}{a_m} \int_L dx \times m_o(x)\, \omega_n^2 \frac{\bar{S}^{(3)}(x,\omega_n)}{a_n} \tag{B-2}$$

Since

$$\int_L dx \times m_o(x)\, \omega_n^2 \frac{\bar{S}^{(3)}(x,\omega_n)}{a_n} = -\omega_n^2 \frac{\bar{S}^{(5)}(\omega_n)}{a_n} I_{55}$$

$$\int_L m_o(x) x dx = 0 \tag{B-3}$$

where

I_{55} = pitch moment of inertia ,

we have

$$\mathrm{Re}\, H_{1,1}(\omega_m,\pm\omega_n) = -\frac{S_c^{(4)}(\omega_m)}{a_m} \omega_n^2 \frac{S_c^{(5)}(\omega_n)}{a_n} I_{55} \pm \frac{S_s^{(4)}(\omega_m)}{a_m} \omega_n^2 \frac{S_s^{(5)}(\omega_n)}{a_n} I_{55} \tag{B-4}$$

$$\mathrm{Im}\, H_{1,1}(\omega_m,\pm\omega_n) = \mp \frac{S_c^{(4)}(\omega_m)}{a_m} \omega_n^2 \frac{S_s^{(5)}(\omega_n)}{a_n} I_{55} - \frac{S_s^{(4)}(\omega_m)}{a_m} \omega_n^2 \frac{S_c^{(5)}(\omega_n)}{a_n} I_{55} \tag{B-5}$$

2) $H_{1,2}$ for I_2

$$I_2 = \mathrm{Re}\left\{\int_L dx \times \sum_{m=1,2} \frac{\bar{S}^{(2)}(x,\omega_m)}{a_m} e^{-i\omega_m t}\right\} \mathrm{Re}\left\{\int_{c(x)} \sum_{n=1,2} \rho \frac{\partial}{\partial t}\left(\frac{\bar{\varphi}_y(\omega_n)}{a_n} e^{-i\omega_n t}\right) dz\right\} \tag{B-6}$$

$$H_{1,2}(\omega_m,\omega_n) = \int_L dx \times \frac{\bar{S}^{(2)}(x,\omega_m)}{a_m} \int_{c(x)} \rho\omega_n \left(\frac{\varphi_{ys}(\omega_n)}{a_n} - i \frac{\varphi_{yc}(\omega_n)}{a_n}\right) dz \tag{B-7}$$

$$\begin{aligned}
\mathrm{Re}\ H_{1,2} = {} & \frac{S_c^{(2)}(\omega_m)}{a_m} \int_L dx \times \rho\omega_n \int_{c(x)} \frac{\varphi_{ys}(\omega_n)}{a_n} dz \\
& + \frac{S_c^{(6)}(\omega_m)}{a_m} \int_L dx\, x^2 \rho\omega_n \int_{c(x)} \frac{\varphi_{ys}(\omega_n)}{a_n} dz \\
& \pm \frac{S_s^{(2)}(\omega_m)}{a_m} \int_L dx \times \rho\omega_n \int_{c(x)} \frac{\varphi_{yc}(\omega_n)}{a_n} dz \\
& \pm \frac{S_s^{(6)}(\omega_m)}{a_m} \int_L dx\, x^2 \rho\omega_n \int_{c(x)} \frac{\varphi_{yc}(\omega_n)}{a_n} dz
\end{aligned} \tag{B-8}$$

$$\begin{aligned}
\mathrm{Im}\ H_{1,2} = {} & \mp \frac{S_c^{(2)}(\omega_m)}{a_m} \int_L dx \times \rho\omega_n \int_{c(x)} \frac{\varphi_{yc}(\omega_n)}{a_n} dz \\
& \mp \frac{S_c^{(6)}(\omega_m)}{a_m} \int_L dx\, x^2 \rho\omega_n \int_{c(x)} \frac{\varphi_{yc}(\omega_n)}{a_n} dz \\
& + \frac{S_s^{(2)}(\omega_m)}{a_m} \int_L dx \times \rho\omega_n \int_{c(x)} \frac{\varphi_{ys}(\omega_n)}{a_n} dz \\
& + \frac{S_s^{(6)}(\omega_m)}{a_m} \int_L dx\, x^2 \rho\omega_n \int_{c(x)} \frac{\varphi_{ys}(\omega_n)}{a_n} dz
\end{aligned} \tag{B-9}$$

3) $H_{1,3}$ for I_3

$$I_3 = \mathrm{Re}\left\{ - \sum_{m=1,2} \frac{\bar{S}^{(4)}(\omega_m)}{a_m} e^{-i\omega_m t} \right\} \mathrm{Re}\left\{ \int_L dx \times \int_{c(x)} (z-z_o) \sum_{n=1,2} \rho \frac{\partial}{\partial t} \left(\frac{\bar{\varphi}_y(\omega_n)}{a_n} e^{-i\omega_n t} \right) dz \right\} \tag{B-10}$$

$$H_{1,3}(\omega_m,\omega_n) = - \frac{\bar{S}^{(4)}(\omega_m)}{a_m} \int_L dx \times \rho\omega_n \int_{c(x)} (z-z_o) \left(\frac{\varphi_{ys}(\omega_n)}{a_n} - i \frac{\varphi_{yc}(\omega_n)}{a_n} \right) dz \tag{B-11}$$

$$\mathrm{Re}\ H_{1,3} = - \frac{S_c^{(4)}(\omega_m)}{a_m} \int_L dx \times \rho\omega_n \int_{c(x)} (z-z_o) \frac{\varphi_{ys}(\omega_n)}{a_n} dz$$

$$\mp \frac{S_s^{(4)}(\omega_m)}{a_m} \int_L dx \times \rho\omega_n \int_{c(x)} (z-z_o) \frac{\varphi_{yc}(\omega_n)}{a_n} dz \tag{B-12}$$

$$\mathrm{Im}\ H_{1,3} = \pm \frac{S_c^{(4)}(\omega_m)}{a_m} \int_L dx \times \rho\omega_n \int_{c(x)} (z-z_o) \frac{\varphi_{yc}(\omega_n)}{a_n} dz$$

$$- \frac{S_s^{(4)}(\omega_m)}{a_m} \int_L dx \times \rho\omega_n \int_{c(x)} (z-z_o) \frac{\varphi_{ys}(\omega_n)}{a_n} dz \tag{B-13}$$

4) $H_{1,4}$ for I_4

$$I_4 = \mathrm{Re}\left\{ \int_L dx \times \sum_{m=1,2} \frac{\bar{S}^{(3)}(x,\omega_m)}{a_m} e^{-i\omega_m t} \right\} \mathrm{Re}\left\{ \int_{c(x)} \rho \sum_{n=1,2} \frac{\partial}{\partial t} \left(\frac{\bar{\varphi}_z(\omega_n)}{a_n} e^{-i\omega_n t} \right) dz \right\} \tag{B-14}$$

$$H_{1,4}(\omega_m,\omega_n) = \int_L dx \times \left(\frac{\bar{S}^{(3)}(\omega_m)}{a_m} - x \frac{\bar{S}^{(5)}(\omega_m)}{a_m} \right) \int_{c(x)} \rho\omega_n \left(\frac{\varphi_{zs}(\omega_n)}{a_n} - i \frac{\varphi_{zc}(\omega_n)}{a_n} \right) dz \tag{B-15}$$

$$\text{Re } H_{1,4} = \frac{S_c^{(3)}(\omega_m)}{a_m} \int_L dx \times \rho\omega_n \int_{c(x)} \frac{\varphi_{zs}(\omega_n)}{a_n} dz$$

$$- \frac{S_c^{(5)}(\omega_m)}{a_m} \int_L dx\, x^2 \rho\omega_n \int_{c(x)} \frac{\varphi_{zs}(\omega_n)}{a_n} dz$$

$$\pm \frac{S_s^{(3)}(\omega_m)}{a_m} \int_L dx \times \rho\omega_n \int_{c(x)} \frac{\varphi_{zc}(\omega_n)}{a_n} dz$$

$$\mp \frac{S_s^{(5)}(\omega_m)}{a_m} \int_L dx\, x^2 \rho\omega_n \frac{\varphi_{zc}(\omega_n)}{a_n} dz \qquad \text{(B-16)}$$

$$\text{Im } H_{1,4} = \mp \frac{S_c^{(3)}(\omega_m)}{a_m} \int_L dx \times \rho\omega_n \int_{c(x)} \frac{\varphi_{zc}(\omega_n)}{a_n} dz$$

$$\pm \frac{S_c^{(5)}(\omega_m)}{a_m} \int_L dx\, x^2 \rho\omega_n \int_{c(x)} \frac{\varphi_{zc}(\omega_n)}{a_n} dz$$

$$+ \frac{S_s^{(3)}(\omega_m)}{a_m} \int_L dx \times \rho\omega_n \int_{c(x)} \frac{\varphi_{zs}(\omega_n)}{a_n} dz$$

$$- \frac{S_s^{(5)}(\omega_m)}{a_m} \int_L dx\, x^2 \rho\omega_n \int_{c(x)} \frac{\varphi_{zs}(\omega_n)}{a_n} dz \qquad \text{(B-17)}$$

5) $H_{1,5}$ for I_5

$$I_5 = \text{Re}\left\{ \sum_{m=1,2} \frac{\bar{S}^{(4)}(\omega_m)}{a_m} e^{-i\omega_m t} \right\} \text{Re}\left\{ \int_L x\, dx \int_{c(x)} y\rho \sum_{n=1,2} \frac{\partial}{\partial t}\left(\frac{\bar{\varphi}_z(\omega_n)}{a_n} e^{-i\omega_n t} \right) dz \right\}$$

(B-18)

$$H_{1,5}(\omega_m, \omega_n) = \frac{\bar{S}^{(4)}(\omega_m)}{a_m} \int_L dx \times \rho\omega_n \int_{c(x)} y \left(\frac{\varphi_{zs}(\omega_n)}{a_n} - i \frac{\varphi_{zc}(\omega_n)}{a_n} \right) dz \qquad \text{(B-19)}$$

$$\text{Re } H_{1,5} = \frac{S_c^{(4)}(\omega_m)}{a_m} \int_L dx \times \rho\omega_n \int_{c(x)} y \frac{\varphi_{zs}(\omega_n)}{a_n} dz$$

$$\pm \frac{S_s^{(4)}(\omega_m)}{a_m} \int_L dx \times \rho\omega_n \int_{c(x)} y \frac{\varphi_{zc}(\omega_n)}{a_n} dz \qquad \text{(B-20)}$$

$$\text{Im } H_{1,5} = \mp \frac{S_c^{(4)}(\omega_m)}{a_m} \int_L dx \times \rho\omega_n \int_{c(x)} y \frac{\varphi_{zc}(\omega_n)}{a_n} dz$$

$$+ \frac{S_s^{(4)}(\omega_m)}{a_m} \int_L dx \times \rho\omega_n \int_{c(x)} y \frac{\varphi_{zs}(\omega_n)}{a_n} dz \qquad \text{(B-21)}$$

6) $H_{1,6}$ for I_6

$$I_6 = \frac{1}{2} \rho \int_L dx \times \int_{c(x)} \text{Re}\left\{ \sum_{m=1,2} \frac{\nabla\bar{\varphi}(\omega_m)}{a_m} e^{-i\omega_m t} \right\} \text{Re}\left\{ \sum_{n=1,2} \frac{\nabla\bar{\varphi}(\omega_n)}{a_n} e^{-i\omega_n t} \right\} dz \qquad \text{(B-22)}$$

$$H_{1,6}(\omega_m, \omega_n) = \frac{1}{2} \rho \int_L dx \times \int_{c(x)} \frac{\nabla\bar{\varphi}(\omega_m)}{a_m} \frac{\nabla\bar{\varphi}(\omega_n)}{a_n} dz \qquad \text{(B-23)}$$

$$\text{Re } H_{1,6} = \frac{\rho}{2} \int_L dx \times \int_{c(x)} \left[\frac{\varphi_{yc}(\omega_m)}{a_m} \frac{\varphi_{yc}(\omega_n)}{a_n} + \frac{\varphi_{zc}(\omega_m)}{a_m} \frac{\varphi_{zc}(\omega_n)}{a_n} \right] dz$$

$$\mp \frac{\rho}{2} \int_L dx \times \int_{c(x)} \left[\frac{\varphi_{ys}(\omega_m)}{a_m} \frac{\varphi_{ys}(\omega_n)}{a_n} + \frac{\varphi_{zs}(\omega_m)}{a_m} \frac{\varphi_{zs}(\omega_n)}{a_n} \right] dz \qquad \text{(B-24)}$$

$$\text{Im } H_{1,6} = \pm \frac{\rho}{2} \int_L dx \times \int_{c(x)} \left[\frac{\varphi_{yc}(\omega_m)}{a_m} \frac{\varphi_{ys}(\omega_n)}{a_n} + \frac{\varphi_{zc}(\omega_m)}{a_m} \frac{\varphi_{zs}(\omega_n)}{a_n} \right] dz$$

$$+ \frac{\rho}{2} \int_L dx \times \int_{c(x)} \left[\frac{\varphi_{ys}(\omega_m)}{a_m} \frac{\varphi_{yc}(\omega_n)}{a_n} + \frac{\varphi_{zs}(\omega_m)}{a_m} \frac{\varphi_{zc}(\omega_n)}{a_n} \right] dz \qquad \text{(B-25)}$$

7) $H_{1,7}$ for I_7

$$I_7 = \frac{1}{2}\rho g \int_L dx \times \left\{ -\mathrm{Re}\left(\sum_{m=1,2} \frac{\bar{r}_+(\omega_m)}{a_m} e^{-i\omega_m t} \right) \mathrm{Re}\left(\sum_{n=1,2} \frac{\bar{r}_+(\omega_n)}{a_n} e^{-i\omega_n t} \right) \right.$$

$$\left. + \mathrm{Re}\left(\sum_{m=1,2} \frac{\bar{r}_-(\omega_m)}{a_m} e^{-i\omega_m t} \right) \mathrm{Re}\left(\sum_{n=1,2} \frac{\bar{r}_-(\omega_n)}{a_n} e^{-i\omega_n t} \right) \right. \quad \text{(B-26)}$$

$$H_{1,7}(\omega_m,\omega_n) = \frac{1}{2}\rho g \int_L dx \times \left\{ -\frac{\bar{r}_+(\omega_m)}{a_m}\frac{\bar{r}_+(\omega_n)}{a_n} + \frac{\bar{r}_-(\omega_m)}{a_m}\frac{\bar{r}_-(\omega_n)}{a_n} \right\} \quad \text{(B-27)}$$

$$\mathrm{Re}\, H_{1,7} = \frac{1}{2}\rho g \int_L dx \times \left\{ -\frac{r_{c+}(\omega_m)}{a_m}\frac{r_{c+}(\omega_n)}{a_n} \pm \frac{r_{s+}(\omega_m)}{a_m}\frac{r_{s+}(\omega_n)}{a_n} \right.$$

$$\left. + \frac{r_{c-}(\omega_m)}{a_m}\frac{r_{c-}(\omega_n)}{a_n} \mp \frac{r_{s-}(\omega_m)}{a_m}\frac{r_{s-}(\omega_n)}{a_n} \right\} \quad \text{(B-28)}$$

$$I_m\, H_{1,7} = \frac{1}{2}\rho g \int_L dx \times \left\{ \mp \frac{r_{c+}(\omega_m)}{a_m}\frac{r_{s+}(\omega_n)}{a_n} - \frac{r_{s+}(\omega_m)}{a_m}\frac{r_{c+}(\omega_n)}{a_n} \right.$$

$$\left. \pm \frac{r_{c-}(\omega_m)}{a_m}\frac{r_{s-}(\omega_n)}{a_n} + \frac{r_{s-}(\omega_m)}{a_m}\frac{r_{c-}(\omega_n)}{a_n} \right\} \quad \text{(B-29)}$$

where evaluation of the r is carried out by using Eqs.(A-30) and (A-31) in Appendix A.

The velocity components of the water on the hull surface as shown in (B-6) - (B-25) are evaluated by using the formula (C-19) in Appendix C.

APPENDIX C

THE RESULTANT POTENTIAL, PRESSURE AND VELOCITY

As indicated in Appendices A and B, we will now evaluate the resultant velocity potentials, the hydrodynamic pressures and velocity components on the hull surface. The resultant potential φ of the water flow due to the ship motion with drift restrained in oblique regular waves consists of the incidence, diffraction and radiation wave potentials. These potential components are evaluated in a stripwise manner described as follows:

Let the incident angle of the wave be designated by μ as shown in Figure 1c and let the wave progress in the positive Y-direction. Then the wave profile is

$$h_I = a \cos(\nu\, y\sin\mu + \nu\, x\cos\mu - \omega t) \qquad (C\text{-}1)$$

where

a = wave amplitude

ν = wave number (ω^2/g)

ω = circular frequency of the wave.

Now, suppose two vertical control planes cut the body at x and x+dx, and observe the wave motion within the fictitiously confined domain which is infinitely extended in the lower half domain, i.e., in y- and z-directions. This domain is designated the "strip domain." The wave equation, Eq.(C-1) can be interpreted in this domain by noting that the term $\nu y\sin\mu$ determines the wave form in the strip domain and that the term $\nu x\cos\mu$ represents the phase shift of the incident wave at $y=0$ and $x=x$ relative to a crest at the origin. Thus the potential of the incident wave, Eq.(C-1) is defined in the strip domain in the form

$$\varphi_I = \frac{ga}{\omega} e^{\nu z} \sin(\nu y \sin\mu + \nu x \cos\mu - \omega t) \quad . \qquad (C\text{-}2)$$

This potential consists of even and odd functions with respect to y and they are expressed in the forms:

$$\varphi_I^o = \frac{ga}{\omega} e^{\nu z} \sin(\nu y \cdot \sin\mu) \cdot \cos(\nu x \cos\mu - \omega t)$$

$$\varphi_I^e = \frac{ga}{\omega} e^{\nu z} \cos(\nu y \cdot \sin\mu) \cdot \sin(\nu x \cos\mu - \omega t) \qquad (C\text{-}3)$$

The odd function is applied to represent the asymmetric flow about the z-axis, while the even function is applied to the symmetric flow. This functional resolution will be utilized in the kinematical boundary conditions in the following section.

Diffracted Wave Potential in a Strip Domain

We assume the diffraction potential in the strip domain in the form

$$\varphi_D^{(m)}(x,y,z;\mu,t)=\mathrm{Re}\left[\int_c Q_D^{(m)}(s)\cdot G(y,z,\eta,\xi)\,ds\; e^{i(\nu x\cos\mu-\omega t)}\right] \qquad (C\text{-}4)$$

where c designates the mean wetted contour of the strip section and m designates the mode of excitation [m=2,3 sway, heave]. $Q_D^{(m)}(s)$ designates the unknown complex source intensities distributed over the strip surface. These source intensities are determined by satisfying the kinematical boundary condition on the body surface

$$\frac{\partial\varphi_D}{\partial n} = -\frac{\partial\varphi_I}{\partial n} \qquad . \qquad (C\text{-}5)$$

These source intensities depend on the mode of excitation, the geometry of the body and the incident wave. The function $G(y,z,\eta,\xi)$ [Reference 20] is the two-dimensional pulsating source potential of unit intensity at the point (η,ξ) in the lower half plane. The exponential term $e^{i\nu x\cos\mu}$ represents the location of the strip $x=x$ where the disturbance occurs in response to the oblique incident wave of wave number ν and incidence μ.

Since, $Q_D^{(m)}$ and G are the complex source intensity and Green's function, respectively, let them be

$$Q_D^{(m)} = Q_{Dr}^{(m)} + iQ_{Di}^{(m)}$$

$$G = G_r - iG_i$$

where $i=\sqrt{-1}$ and where $Q_{Dr}^{(m)}$ and $Q_{Di}^{(m)}$ are real and imaginary parts of $Q_D^{(m)}$, and G_r and $-G_i$ are real and imaginary parts of G.

Equation (C-4) is then changed to

$$\varphi_D^{(m)} = \int_c \left(Q_{Dr}^{(m)}G_r + Q_{Di}^{(m)}G_i\right)ds\cdot\cos(\nu x\cos\mu-\omega t)$$

$$-\int_c \left(-Q_{Dr}^{(m)}G_i + Q_{Di}^{(m)}G_r\right)ds\cdot\sin(\nu x\cos\mu-\omega t) \qquad . \qquad (C\text{-}6)$$

This potential $\varphi_D^{(m)}$ is determined by satisfying the kinematical boundary condition, Eq.(C-5), which becomes

$$\frac{\partial \varphi_D^{(2)}}{\partial n} = -\frac{\partial \varphi_I^{o}}{\partial n}$$

$$\frac{\partial \varphi_D^{(3)}}{\partial n} = -\frac{\partial \varphi_I^{e}}{\partial n} \qquad \text{(C-7)}$$

on the fixed body surface. This boundary condition is specifically written in the following forms by dropping the suffix D, i.e., for sway (m=2),

$$\sum_{j=1}^{N} Q_j^{(2)} I_{ij}^{(2)} + \sum_{j=1}^{N} Q_{N+j}^{(2)} J_{ij}^{(2)} =$$

$$-\omega e^{\nu z_i}[\sin\mu \cdot \cos(\nu y_i \sin\mu)\sin\alpha_i - \sin(\nu y_i \sin\mu)\cos\alpha_i]$$

$$-\sum_{j=1}^{N} Q_j^{(2)} J_{ij}^{(2)} - \sum_{j=1}^{N} Q_{N+j}^{(2)} I_{ij}^{(2)} = 0 \qquad \text{(C-8)}$$

and, for heave-exciting (m=3),

$$\sum_{j=1}^{N} Q_j^{(3)} I_{ij}^{(3)} + \sum_{j=1}^{N} Q_{N+j}^{(3)} J_{ij}^{(3)} = 0$$

$$-\sum_{j=1}^{N} Q_j^{(3)} J_{ij}^{(3)} + \sum_{j=1}^{N} Q_{N+j}^{(3)} I_{ij}^{(3)} =$$

$$-\omega e^{\nu z_i}[\sin\mu \cdot \sin(\nu y_i \sin\mu)\sin\alpha_i + \cos(\nu y_i \sin\mu)\cos\alpha_i] \quad . \qquad \text{(C-9)}$$

Here α_i is the angle made between i^{th} segment and the positive x-axis and both $I_{ij}^{(m)}$ and $J_{ij}^{(m)}$ formally represent the normal derivatives $\frac{\partial}{\partial n}\int_c G_r ds$ and $\frac{\partial}{\partial n}\int_c G_i ds$, and are called the "influence coefficients" with specific definitions given in the Appendix of Reference ; and $Q_j^{(m)} = Q_r^{(m)}$ and $Q_{N+j} = Q_i^{(m)}$ at the j^{th} segment. If N sources are distributed over the strip surface, we obtain a (2N x 2N) simultaneous equation system with 2N unknowns, i.e., the real and imaginary parts of the N sources.

Since the right-hand sides of Eqs.(C-8) and (C-9) represent the expression

$\frac{1}{a}\frac{\partial \varphi_I}{\partial n}$, the solution $Q_D^{(m)}$ gives the source intensity per unit amplitude of the incident wave and the insertion of this $Q_D^{(m)}$ in Eq.(C-6) then provides the diffraction potential per unit amplitude of the incident wave $\frac{1}{a}\varphi_D^{(m)}$.

In reference to (C-6), the complex diffraction potential $\bar{\varphi}_D/a$ in the strip domain is defined by its real and imaginary components $\varphi_{Dc}^{(m)}/a$ and $\varphi_{Ds}^{(m)}/a$ in the following forms:

$$\frac{\varphi_{Dc}^{(m)}}{a} = \frac{\Phi_{Dc}^{(m)}}{a}\cos(\nu x\cos\mu) - \frac{\Phi_{Ds}^{(m)}}{a}\sin(\nu x\cos\mu)$$

$$\frac{\varphi_{Ds}^{(m)}}{a} = \frac{\Phi_{Dc}^{(m)}}{a}\sin(\nu x\cos\mu) + \frac{\Phi_{Ds}^{(m)}}{a}\cos(\nu x\cos\mu) \qquad \text{(C-10)}$$

with

$$\frac{\Phi_{Dc}^{(m)}}{a} = \int_c (Q_{Dr}^{(m)} G_r + Q_{Di}^{(m)} G_i)\,ds$$

$$\frac{\Phi_{Ds}^{(m)}}{a} = \int_c (-Q_{Dr}^{(m)} G_i + Q_{Di}^{(m)} G_r)\,ds \quad . \qquad \text{(C-11)}$$

The Radiation Potential in the Strip Domain

From the solutions of the coupled heaving and pitching, and the coupled swaying, rolling and yawing motions of a ship in oblique seas, according to a procedure for motion calculation, we obtain the five responses $S^{(m)}$. The displacements of the section consist of three degrees of freedom: sway, heave and roll which are induced by the motion of the ship, namely,

$$S^{(2)}(x) = S^{(2)} + xS^{(6)}$$

$$S^{(3)}(x) = S^{(3)} - xS^{(5)}$$

and

$$S^{(4)}(x) = S^{(4)} \quad . \qquad \text{(C-12)}$$

The complex radiation potential $\bar{\varphi}_R^{(m)}/a$ which is due to the actual response motion of the section in the incident wave is given by the following

expressions:

$$\frac{\varphi_{Rc}^{(m)}}{a} = \frac{S_c^{(m)}}{a}\Phi_{Rc}^{(m)} - \frac{S_s^{(m)}}{a}\Phi_{Rs}^{(m)}$$

$$\frac{\varphi_{Rs}^{(m)}}{a} = \frac{S_c^{(m)}}{a}\Phi_{Rs}^{(m)} + \frac{S_s^{(m)}}{a}\Phi_{Rc}^{(m)} \qquad \text{(C-13)}$$

with

$$\Phi_{Rc}^{(m)} = \int_c (Q_r^{(m)} G_r + Q_i^{(m)} G_i)\, ds$$

$$\Phi_{Rs}^{(m)} = \int_c (-Q_r^{(m)} G_i + Q_i^{(m)} G_r)\, ds \quad . \qquad \text{(C-14)}$$

The $\Phi_R^{(m)}$ in the above presents the radiation potential per unit motion displacement, i.e., $S_c^{(m)} = 1$ and $S_s^{(m)} = 0$. It is to be noted that the sway displacement $\bar{S}^{(2)}$ has to be replaced by $\bar{S}^{(2)} + z_o\bar{S}^{(4)}$ when the rolling axis passes through the origin 0 which is defined in Figure 1-b. Since the section motion displacement $\bar{S}^{(m)}$ is induced by the ship motion, $\bar{S}^{(2)}$ and $\bar{S}^{(3)}$ should satisfy Eq.(C-12).

In view of the above, the resultant velocity potential $\bar{\varphi}/a$ for each section is given by the following expressions:

$$\frac{\varphi_c}{a} = \frac{g}{\omega} e^{\nu z}\sin[\nu(y\sin\mu + x\cos\mu)]$$

$$+ \sum_{m=2,3}\left[\frac{\Phi_{Dc}^{(m)}}{a}\cos(\nu x\cos\mu) - \frac{\Phi_{Ds}^{(m)}}{a}\sin(\nu x\cos\mu)\right]$$

$$+ \sum_{m=2,3,4}\left(\frac{S_c^{(m)}(x)}{a}\Phi_{Rc}^{(m)} - \frac{S_s^{(m)}(x)}{a}\Phi_{Rs}^{(m)}\right)$$

$$\frac{\varphi_s}{a} = -\frac{g}{\omega} e^{\nu z}\cos[\nu(y\sin\mu + x\cos\mu)]$$

$$+ \sum_{m=2,3}\left[\frac{\Phi_{Dc}^{(m)}}{a}\sin(\nu x\cos\mu) + \frac{\Phi_{Ds}^{(m)}}{a}\cos(\nu x\cos\mu)\right]$$

$$+ \sum_{m=2,3,4}\left(\frac{S_c^{(m)}(x)}{a}\Phi_{Rs}^{(m)} + \frac{S_s^{(m)}(x)}{a}\Phi_{Rc}^{(m)}\right) \quad . \qquad \text{(C-15)}$$

The Hydrodynamic Pressure

The complex resultant hydrodynamic pressure $\frac{\bar{p}}{a}$ per unit wave amplitude is derived from the potential $\frac{\varphi_c}{a}$ and $\frac{\varphi_s}{a}$, as the following:

$$\frac{p_c}{a} = -\rho\omega\frac{\varphi_s}{a} \quad ; \quad \frac{p_s}{a} = \rho\omega\frac{\varphi_c}{a} \quad . \tag{C-16}$$

Substituting Eqs.(C-15) into Eq.(C-16), we have

$$\frac{p_c}{a} = \frac{p_{Kc}^{(3)}}{a}\cos(\nu x\cos\mu) - \frac{p_{Ks}^{(2)}}{a}\sin(\nu x\cos\mu)$$

$$+ \sum_{m=2,3}\left[\frac{p_{Dc}^{(m)}}{a}\cos(\nu x\cos\mu) - \frac{p_{Ds}^{(m)}}{a}\sin(\nu x\cos\mu)\right]$$

$$+ \sum_{m=2,3,4}\left(\frac{S_c^{(m)}(x)}{a}p_{Rc}^{(m)} - \frac{S_s^{(m)}(x)}{a}p_{Rs}^{(m)}\right)$$

$$\frac{p_s}{a} = \frac{p_{Kc}^{(3)}}{a}\sin(\nu x\cos\mu) + \frac{p_{Ks}^{(2)}}{a}\cos(\nu x\cos\mu)$$

$$+ \sum_{m=2,3}\left[\frac{p_{Dc}^{(m)}}{a}\sin(\nu x\cos\mu) + \frac{p_{Ds}^{(m)}}{a}\cos(\nu x\cos\mu)\right]$$

$$+ \sum_{m=2,3,4}\left(\frac{S_c^{(m)}(x)}{a}p_{Rs}^{(m)} + \frac{S_s^{(m)}(x)}{a}p_{Rc}^{(m)}\right) \tag{C-17}$$

with

$$\frac{p_{Kc}^{(2)}}{a} = 0 \quad , \quad \frac{p_{Ks}^{(2)}}{a} = \rho g e^{\nu z}\sin(\nu y\sin\mu)$$

$$\frac{p_{Kc}^{(3)}}{a} = \rho g e^{\nu z}\cos(\nu y\sin\mu) \quad , \quad \frac{p_{Ks}^{(3)}}{a} = 0$$

$$\frac{p_{Dc}^{(m)}}{a} = -\rho\omega\frac{\Phi_{Ds}^{(m)}}{a} \quad , \quad \frac{p_{Ds}^{(m)}}{a} = \rho\omega\frac{\Phi_{Dc}^{(m)}}{a}$$

$$p_{Rc}^{(m)} = -\rho\omega\,\Phi_{Rs}^{(m)} \quad , \quad p_{Rs}^{(m)} = \rho\omega\,\Phi_{Rc}^{(m)} \quad . \tag{C-18}$$

(C-19) in Appendix C.

The Velocity Components

The velocity components are derived from the potential Eqs.(C-15) in the following form:

$$\frac{\partial}{\partial y}\frac{\varphi_c}{a} = \omega\, e^{\nu z}\sin\mu\,\cos[\nu(y\sin\mu + x\cos\mu)]$$

$$+ \sum_{m=2,3}\left[\frac{\partial}{\partial y}\frac{\Phi^{(m)}_{Dc}}{a}\cos(\nu x\cos\mu) - \frac{\partial}{\partial y}\frac{\Phi^{(m)}_{Ds}}{a}\sin(\nu x\cos\mu)\right]$$

$$+ \sum_{m=2,3,4}\left(\frac{S^{(m)}_c}{a}\frac{\partial}{\partial y}\Phi^{(m)}_{Rc} - \frac{S^{(m)}_s}{a}\frac{\partial}{\partial y}\Phi^{(m)}_{Rs}\right)$$

$$\frac{\partial}{\partial z}\frac{\varphi_c}{a} = \omega\, e^{\nu z}\sin[\nu(y\sin\mu + x\cos\mu)]$$

$$+ \sum_{m=2,3}\left[\frac{\partial}{\partial z}\frac{\Phi^{(m)}_{Dc}}{a}\cos(\nu x\cos\mu) - \frac{\partial}{\partial z}\frac{\Phi^{(m)}_{Ds}}{a}\sin(\nu x\cos\mu)\right]$$

$$+ \sum_{m=2,3,4}\left(\frac{S^{(m)}_c(x)}{a}\frac{\partial}{\partial z}\Phi^{(m)}_{Rc} - \frac{S^{(m)}_s(x)}{a}\frac{\partial}{\partial z}\Phi^{(m)}_{Rs}\right)$$

$$\frac{\partial}{\partial y}\frac{\varphi_s}{a} = \omega\, e^{\nu z}\sin\mu\sin[\nu(y\sin\mu + x\cos\mu]$$

$$+ \sum_{m=2,3}\left[\frac{\partial}{\partial y}\frac{\Phi^{(m)}_{Dc}}{a}\sin(\nu x\cos\mu) + \frac{\partial}{\partial y}\frac{\Phi^{(m)}_{Ds}}{a}\cos(\nu x\cos\mu)\right]$$

$$+ \sum_{m=2,3,4}\left(\frac{S^{(m)}_c(x)}{a}\frac{\partial}{\partial y}\Phi^{(m)}_{Rc} + \frac{S^{(m)}_s(x)}{a}\frac{\partial}{\partial y}\Phi^{(m)}_{Rc}\right)$$

$$\frac{\partial}{\partial z}\frac{\varphi_s}{a} = -\omega\, e^{\nu z}\cos[\nu(y\sin\mu + x\cos\mu)]$$

$$+ \sum_{m=2,3}\left[\frac{\partial}{\partial z}\frac{\Phi^{(m)}_{Dc}}{a}\sin(\nu x\cos\mu) + \frac{\partial}{\partial z}\frac{\Phi^{(m)}_{Ds}}{a}\cos(\nu x\cos\mu)\right]$$

$$+ \sum_{m=2,3,4}\left(\frac{S^{(m)}_c(x)}{a}\frac{\partial}{\partial z}\Phi^{(m)}_{Rs} + \frac{S^{(m)}_s(x)}{a}\frac{\partial}{\partial z}\Phi^{(m)}_{Rc}\right) \quad . \qquad \text{(C-19)}$$

Formulas (A-30) and (A-31) are evaluated by employing (C-17) in Appendix C.

The velocity components due to the radiation and diffraction potentials Φ_R and Φ_D In Eqs.(C-19) are calculated by using the formulas (C-10), (C-11) and (C-14) and the formulas for the velocity component due to the source potential per unit intensity in Appendix D. Also, the symbols x and y used in Appendix D are identical to y and z.

$$- \frac{S_s^{(4)}(\omega_m)}{a_m} \omega_n^2 \frac{S_c^{(5)}(\omega_n)}{a_n} I_{55} \qquad (B\text{-}5)$$

APPENDIX D

THE VELOCITY COMPONENTS DUE TO THE UNIT PULSATING SOURCE[19]

The velocity components due to the unit pulsating source ($G=G_r-iG_i$) along the cylinder contour are evaluated by applying Frank's closed-fit method.[20] The fluid velocity components at the i^{th} midpoint (x_i,y_i) due to the source on a segment S_j for mode m are

$$\begin{aligned}
\frac{\partial}{\partial x} \text{Re}\{G_r\} &= \text{Re}\left\{\frac{dG_r}{dz}\right\} \\
\frac{\partial}{\partial x} \text{Re}\{G_i\} &= \text{Re}\left\{\frac{dG_i}{dz}\right\} \\
\frac{\partial}{\partial y} \text{Re}\{G_r\} &= -\text{Im}\left\{\frac{dG_r}{dz}\right\} \\
\frac{\partial}{\partial y} \text{Re}\{G_i\} &= -\text{Im}\left\{\frac{dG_i}{dz}\right\}
\end{aligned} \qquad (D\text{-}1)$$

where

$$G_r = \int_{S_j} \left[\log(z_i-\zeta) - \log(z_i-\bar{\zeta}) + 2P.V. \int_0^\infty \frac{e^{-ik(z_i-\zeta)}}{\nu - k}\, dk\right] ds$$

$$- (-1)^m \int_{-S_j} \left[\log(z_i+\bar{\zeta}) - \log(z_i+\zeta) + 2P.V. \int_0^\infty \frac{e^{-ik(z_i+\zeta)}}{\nu - k}\, dk\right] ds$$

$$G_i = 2\pi \int_{S_j} e^{-i\nu(z_i-\bar{\zeta})}\, ds - (-1)^m 2\pi \int_{S_j} e^{-i\nu(z_i+\zeta)}\, ds$$

The complex velocities, in (D-1), are:

$$\frac{dG_r}{dz} = \int_{S_j} \left[\frac{1}{z_i-\zeta} + \frac{1}{z_i-\bar{\zeta}} - 2i\nu P.V. \int_0^\infty \frac{e^{-ik(z_i-\bar{\zeta})}}{\nu - k}\, dk\right] ds$$

$$- (-1)^m \int_{S_j} \left[\frac{1}{z_i+\zeta} + \frac{1}{z_i+\zeta} - 2i\nu P.V. \int_0^\infty \frac{e^{-ik(z_i+\zeta)}}{\nu - k}\, dk\right] ds \qquad (D\text{-}2)$$

$$+ \frac{S_s^{(6)}(\omega_m)}{a_m} \int_L dx\, x^2 \rho \omega_n \int_{c(x)} \frac{\varphi_{ys}(\omega_n)}{a_n} dz \qquad \text{(B-9)}$$

$$\frac{dG_i}{dz} = -2\pi i\nu \int_{S_j} e^{-i\nu(z_i-\bar{\zeta})}\, ds + (-1)^m 2\pi i\nu \int_{S_{-j}} e^{-i\nu(z_i+\zeta)} ds \qquad \text{(D-3)}$$

Making use of the relation (α = slope of the segment)

$$d\zeta = ds e^{i\alpha}$$

$$d\bar{\zeta} = ds e^{-i\alpha}$$

we evaluate the above integral with respect to S;

$$\int_{S_j} \frac{ds}{z_i - \zeta} = \int_{S_j} \frac{d\zeta\, e^{-i\alpha_j}}{z_i - \zeta}$$

$$= -(\cos\alpha_j - i\sin\alpha_j) \left[\log(z_i-\zeta)\right]_{\zeta_j}^{\zeta_{j+1}}$$

$$= (\cos\alpha_j - i\sin\alpha_j) \left[\log \sqrt{(x_i-\xi_j)^2 + (y_i-\eta_j)^2}\right.$$

$$\left. - \log \sqrt{(x_i-\xi_{j+1})^2 + (y_i-\eta_{j+1})^2}\right)$$

$$\left. + i\left(\tan^{-1} \frac{y_i-\eta_j}{x_i-\xi_j} - \tan^{-1} \frac{y_i-\eta_{j+1}}{x_i-\xi_{j+1}}\right)\right] \qquad \text{(D-4)}$$

Separating the above into real and imaginary parts,

$$\mathrm{Re}\left\{\int_{S_j} \frac{ds}{z_i-\zeta}\right\} = \cos\alpha_j \left[\log \sqrt{(x_i-\xi_j)^2 + (y_i-\eta_j)^2} - \log \sqrt{(x_i-\xi_{j+1})^2 + (y_i-\eta_{j+1})^2}\right]$$

$$+ \sin\alpha_j \left[\tan^{-1} \frac{y_i-\eta_j}{x_i-\xi_j} - \tan^{-1} \frac{y_i-\eta_{j+1}}{x_i-\xi_{j+1}}\right]$$

$$\mathrm{Im}\left\{\int_{S_j}\frac{ds}{z_i-\bar{\xi}}\right\} = \cos\alpha_j\left[\tan^{-1}\frac{y_i-\eta_j}{x_i-\xi_j} - \tan^{-1}\frac{y_i-\eta_{j+1}}{x_i-\xi_{j+1}}\right]$$

$$- \sin\alpha_j\left[\log\sqrt{(x_i-\xi_j)^2+(y_i-\xi_j)^2} - \log\sqrt{(x_i-\xi_{j+1})^2+(y_i-\eta_{j+1})^2}\right]$$

$$\mathrm{Re}\left\{\int_{S_j}\frac{ds}{z_i-\bar{\zeta}}\right\} = \cos\alpha_j\left[\log\sqrt{(x_i-\xi_j)^2+(y_i+\eta_j)^2} - \log\sqrt{(x_i-\xi_{j+1})^2+(y_i+\eta_{j+1})^2}\right]$$

$$- \sin\alpha_j\left[\tan^{-1}\frac{y_i+\eta_j}{x_i-\xi_j} - \tan^{-1}\frac{y_i+\eta_{j+1}}{x_i-\xi_{j+1}}\right]$$

$$\mathrm{I_m}\left\{\int_{S_j}\frac{ds}{z_i-\bar{\zeta}}\right\} = \cos\alpha_j\left[\tan^{-1}\frac{y_i+\eta_j}{x_i-\xi_j} - \tan^{-1}\frac{y_i+\eta_{j+1}}{x_i-\xi_{j+1}}\right]$$

$$+ \sin\alpha_j\left[\log\sqrt{(x_i-\xi_j)^2+(y_i+\eta_j)^2} - \log\sqrt{(x_i-\xi_{j+1})^2+(y_i+\eta_{j+1})^2}\right]$$

The Cauchy-Principle value integral is given by (D-5)

$$2i\nu\int_{S_j} ds \int_0^\infty \frac{e^{-ik(z-\bar{\zeta})}}{k-\nu}\,dk$$

$$= -2(\cos\alpha_j+i\sin\alpha_j)\left\{\left[\log\sqrt{(x_i-\xi_j)^2+(y_i+\eta_j)^2} - \log\sqrt{(x_i-\xi_{j+1})^2+(y_i+\eta_{j+1})^2}\right.\right.$$

$$+ \int_0^\infty \frac{e^{(y_i+\eta_{j+1})k}\cos k(x_i-\xi_{j+1})}{\nu-k}\,dk - \int_0^\infty \frac{e^{(y_i+\eta_j)k}\cos k(x_i-\xi_j)}{\nu-k}\,dk\Big]$$

$$+ i\left[\tan^{-1}\frac{y_i+\eta_j}{x_i-\xi_j} - \tan^{-1}\frac{y_i+\eta_{j+1}}{x_i-\xi_{j+1}} - \int_0^\infty \frac{e^{(y_i+\eta_{j+1})k}\sin k(x_i-\xi_{j+1})}{\nu-k}\,dk\right.$$

$$\left.\left.+ \int_0^\infty \frac{e^{(y_i+\eta_j)k}\sin k(x_i-\xi_j)}{\nu-k}\,dk\right]\right\} \qquad (D\text{-}6)$$

$$H_{1,5}(\omega_m,\omega_n) = \frac{\tau_{m'}}{a_m}\int_L dx \times \rho\omega_n \int_{c(x)} y\left(\frac{\tau_{zs}\tau_{n'}}{a_n} - i\frac{\tau_{zc}\tau_{n'}}{a_n}\right)dz \qquad \text{(B-19)}$$

The first integral in (D-2) and (D-3) is

$$\int_{S_j} -i\nu e^{-i\nu(z_i-\bar{\zeta})}\,ds$$

$$= -i\nu e^{i\alpha_j}\int_{S_j} e^{-i\nu(z_i-\bar{\zeta})}\,d\bar{\zeta}$$

$$= -e^{\nu(y_i+\eta_{j+1})}(\cos[\alpha_j-\nu(x_i-\xi_{j+1})] + i\sin[\alpha_j-\nu(x_i-\xi_{j+1})])$$

$$+ e^{\nu(y_i+\eta_j)}(\cos[\alpha_j-\nu(x_i-\xi_j)] + i\sin[\alpha_j-\nu(x_i-\xi_j)]) \qquad \text{(D-7)}$$

Separating the above into the real and imaginary parts, we have,

$$\mathrm{Re}\left\{\int_{S_j} -i\nu e^{-i\nu(z_i-\bar{\zeta})}\,ds\right\}$$

$$= e^{\nu(y_i+\eta_j)}\cos[\alpha_j-\nu(x_i-\xi_j)] - e^{\nu(y_i+\eta_{j+1})}\cos[\alpha_j-\nu(x_i-\xi_{j+1})]$$

$$\mathrm{Im}\left\{\int_{S_j} -i\nu e^{-i\nu(z_i-\bar{\zeta})}\,ds\right\}$$

$$= -e^{\nu(y_i+\eta_j)}\sin[\nu(x_i-\xi_y)-\alpha_j] + e^{\nu(y_i+\eta_{j+1})}\sin[\nu(x_i-\xi_{j+1})-\alpha_j]$$

(D-8)